

Prospects for blind CMB B-modes reconstruction in future experiments

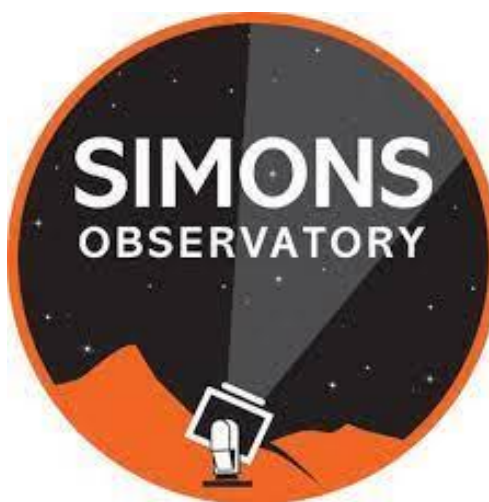
Alessandro Carones

alessandro.carones@roma2.infn.it



TOR VERGATA
UNIVERSITY OF ROME

CMB EXPERIMENTS



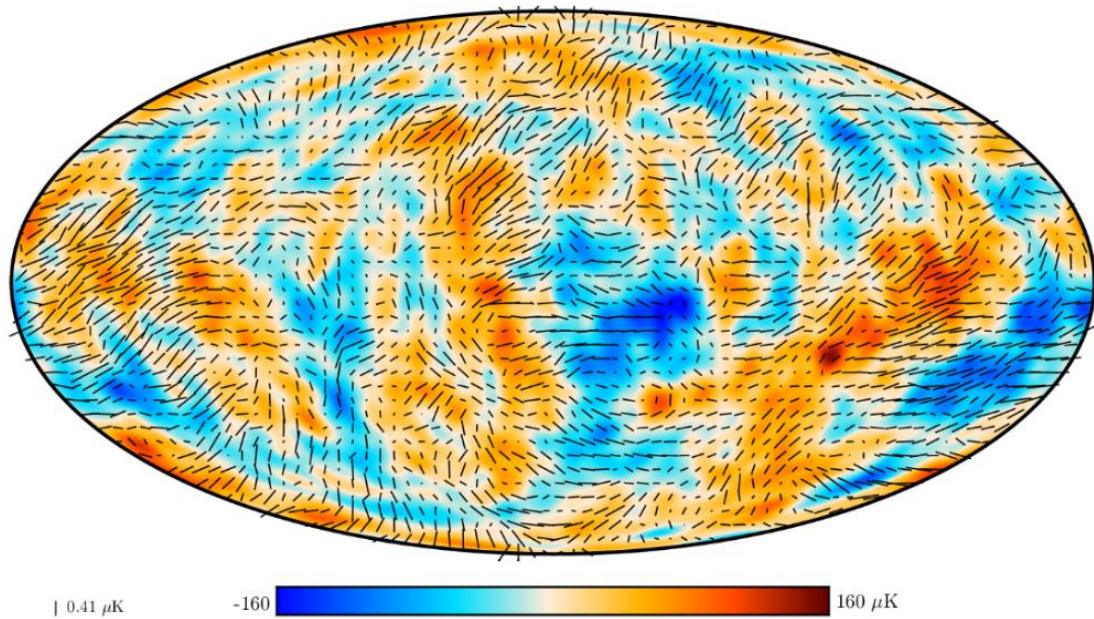
Present

2023

2030s

CMB POLARIZATION

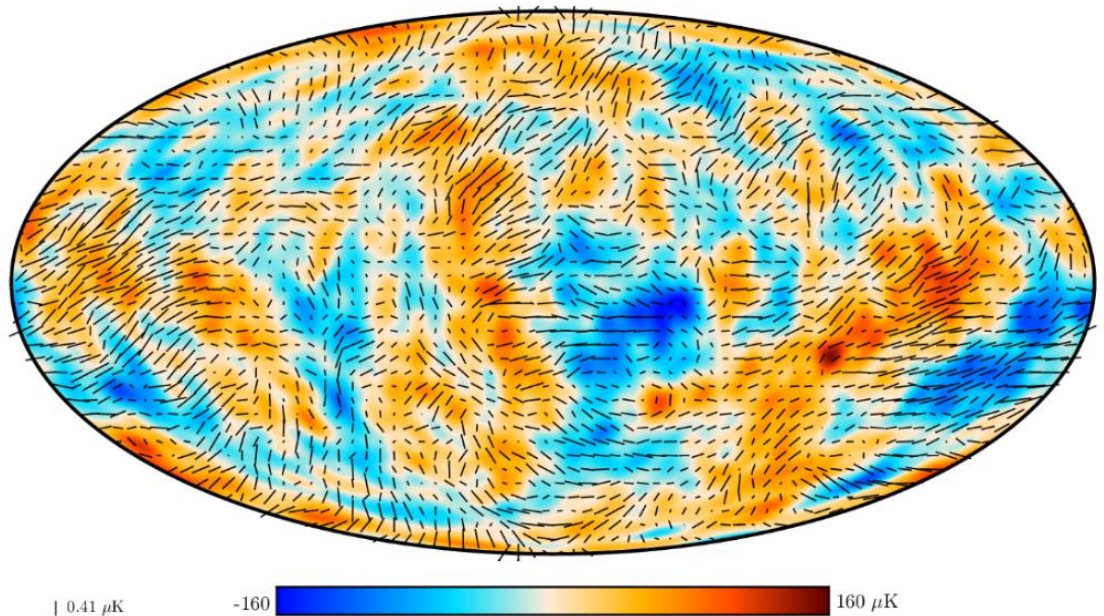
(Planck Collaboration)



$$P_{\pm} = Q \pm iU = \sum_{\ell m} a_{\pm 2, \ell m} Y_{\ell m}^{\pm 2}$$
$$a_{\ell m}^E = -\frac{1}{2}(a_{2, \ell m} + a_{-2, \ell m})$$
$$\begin{array}{c} \diagup \quad \diagdown \\ \text{---} \quad \text{---} \\ \diagdown \quad \diagup \end{array} \quad E < 0$$
$$a_{\ell m}^B = -\frac{1}{2i}(a_{2, \ell m} - a_{-2, \ell m})$$
$$\begin{array}{c} \diagup \quad \diagdown \\ \text{---} \quad \text{---} \\ \diagdown \quad \diagup \end{array} \quad B < 0$$
$$\begin{array}{c} \diagup \quad \diagdown \\ \text{---} \quad \text{---} \\ \diagdown \quad \diagup \end{array} \quad E > 0$$
$$\begin{array}{c} \diagup \quad \diagdown \\ \text{---} \quad \text{---} \\ \diagdown \quad \diagup \end{array} \quad B > 0$$

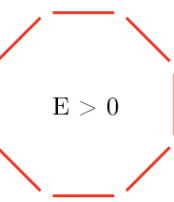
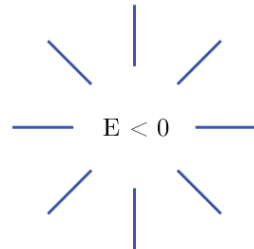
CMB POLARIZATION

(Planck Collaboration)

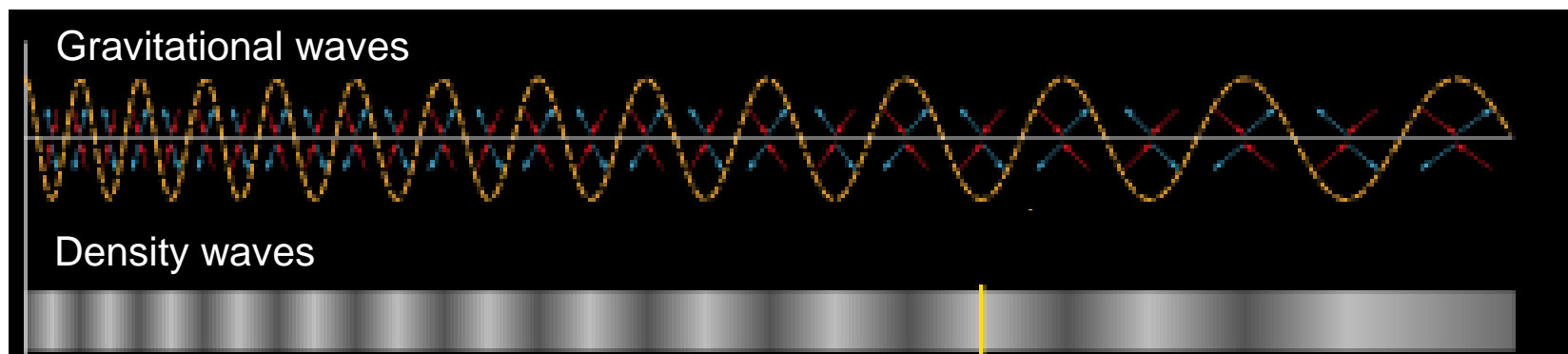
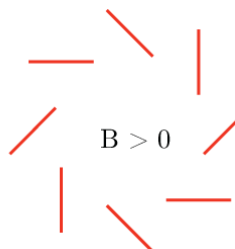
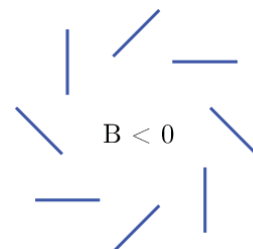


$$P_{\pm} = Q \pm iU = \sum_{\ell m} a_{\pm 2, \ell m} Y_{\ell m}^{\pm 2}$$

$$a_{\ell m}^E = -\frac{1}{2}(a_{2, \ell m} + a_{-2, \ell m})$$



$$a_{\ell m}^B = -\frac{1}{2i}(a_{2, \ell m} - a_{-2, \ell m})$$

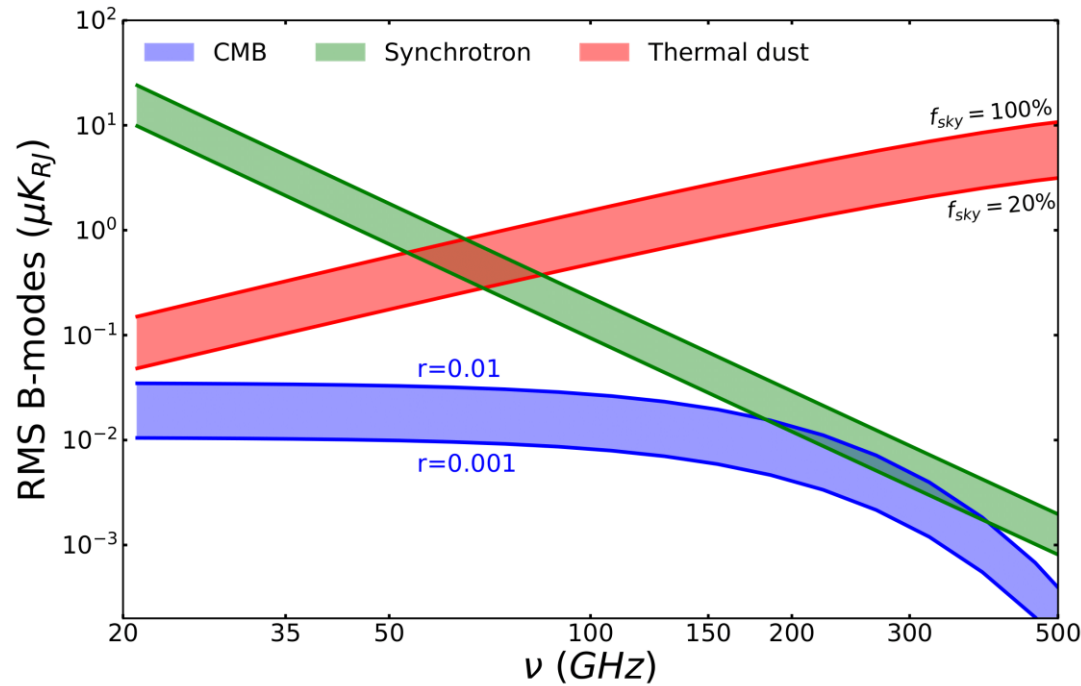


**E-modes
B-modes**

E-modes

GALACTIC FOREGROUNDS

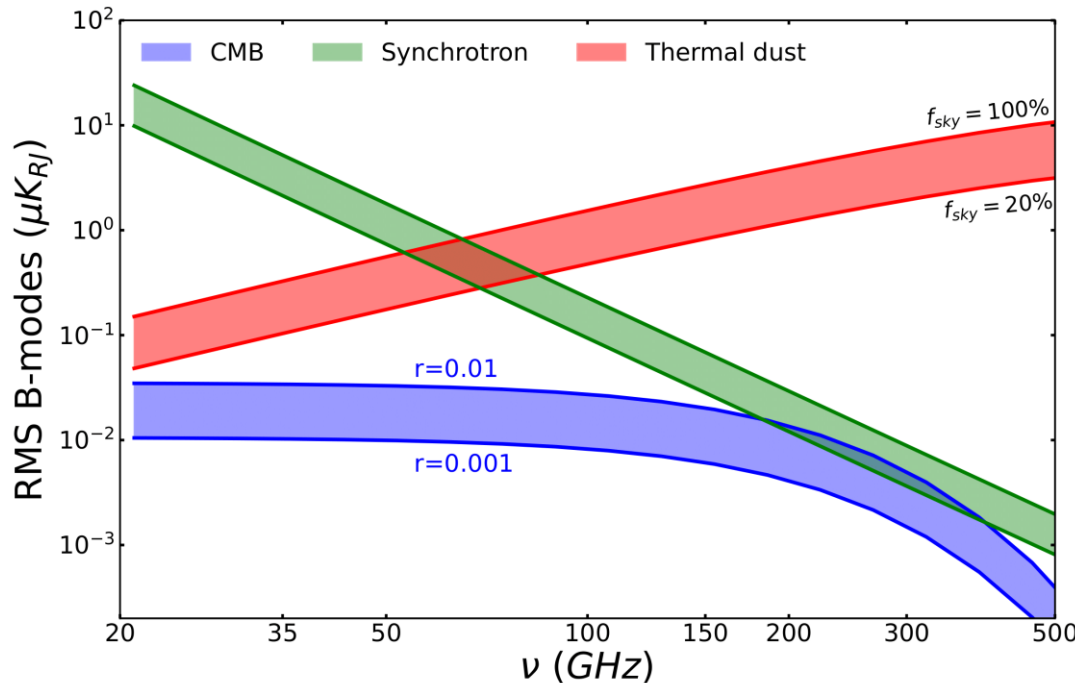
(see Frolov's talk)



$$r = \frac{A_T}{A_S} < 0.028$$

(Galloni et al., 2022)

GALACTIC FOREGROUNDS



$$r = \frac{A_T}{A_S} < 0.028$$

(Galloni et al., 2022)

$$\{Q, U\}_s(\nu, p) = \{Q, U\}_s(\nu_s, p) \cdot \left(\frac{\nu}{\nu_s}\right)^{\beta_s(p)}$$

$$\{Q, U\}_d(\nu, p) = \{Q, U\}_d(\nu_d, p) \cdot \left(\frac{\nu}{\nu_d}\right)^{\beta_d(p)+1} \frac{B(\nu, T_d(p))}{B(\nu_d, T_d(p))}$$

Commonly used PySM (Zonca et al., 2021) models:

- ***s0*: constant spectral index**
- ***s1*: anisotropic spectral index across the sky**
- ***d0*: constant spectral parameters**
- ***d1*: anisotropic spectral parameters across the sky**

FOREGROUND SUBTRACTION

(Bennett *et al.*, 2003)

Internal Linear Combination (ILC)

$$d_i(p) = a_i s_{\text{CMB}}(p) + f_i(p) + n_i(p)$$

$$\hat{s}_{\text{ILC}}(p) = \sum_i \omega_i \cdot d_i(p) \quad \text{with} \quad \sum_i \omega_i \cdot a_i = 1$$

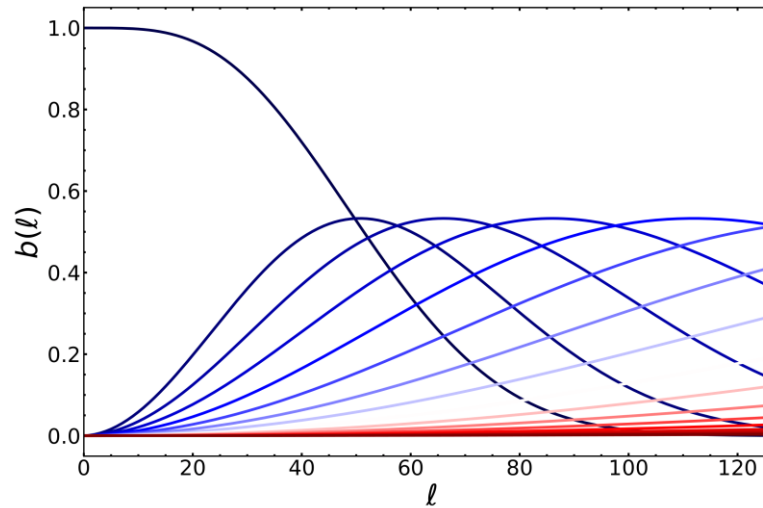
$$\hat{s}_{\text{ILC}}(p) = s_{\text{CMB}}(p) + \sum_i \omega_i \cdot (f_i(p) + n_i(p))$$

Global variance minimization

$$\langle \hat{s}_{\text{ILC}}^2 \rangle = \langle \hat{s}_{\text{CMB}}^2 \rangle + \sum_{i,i'} \omega_i (F_{ii'} + N_{ii'}) \omega_{i'}$$

NEEDLET ILC (NILC)

- Needlets are a particular wavelet system which guarantees simultaneous localization in harmonic and pixel space



(Delabrouille et al., 2009)

- NILC CMB solution is obtained by linearly combining maps at different frequencies at each needlet scale minimizing the variance of the output

$$\beta_j^i(\hat{n}) = \sum_{\ell m} (a_{\ell m}^{B,i} \cdot b_j(\ell)) \cdot Y_{\ell m}(\hat{n}),$$

$$\beta_j^{NILC}(\hat{n}) = \sum_i w_j^i(\hat{n}) \cdot \beta_j^i(\hat{n}),$$

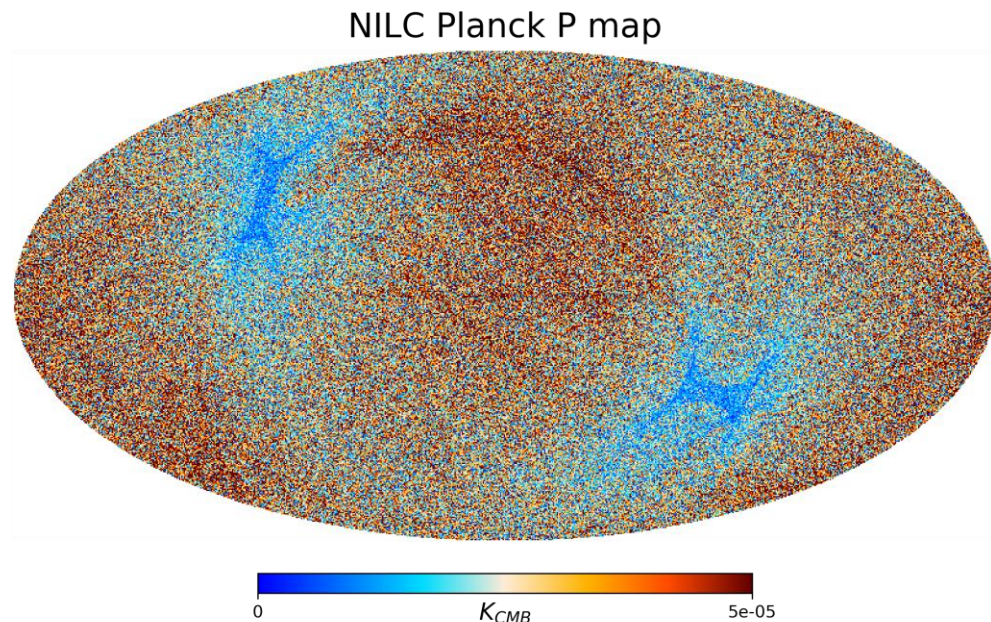
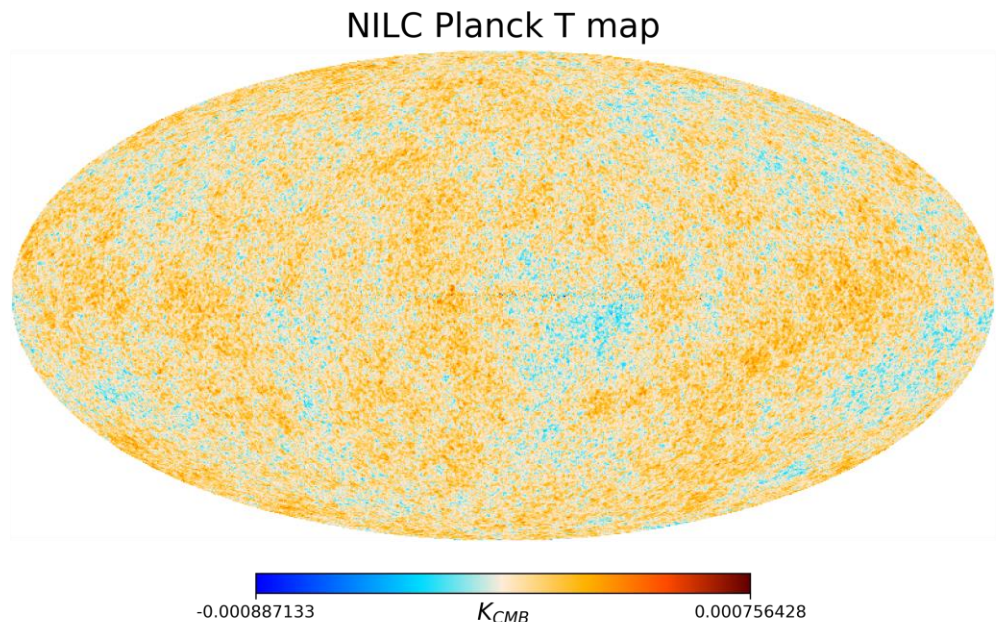
$$w_j^i(\hat{n}) = \frac{\sum_{ik} C_{ik}^{(j)-1}(\hat{n})}{\sum_{zk} C_{zk}^{(j)-1}(\hat{n})},$$

$$C_{ik}^{(j)}(\hat{n}) = \frac{1}{N_p} \sum_{p \in \wp(\hat{n})} W(p) \cdot (\beta_j^i(p) \cdot \beta_j^k(p))$$

NILC FOR PLANCK

- NILC successfully applied to Planck CMB data

(*Planck Collaboration*)



- But:
 - It cannot be consistently applied to partial-sky polarization data from sub-orbital experiments with its current implementation

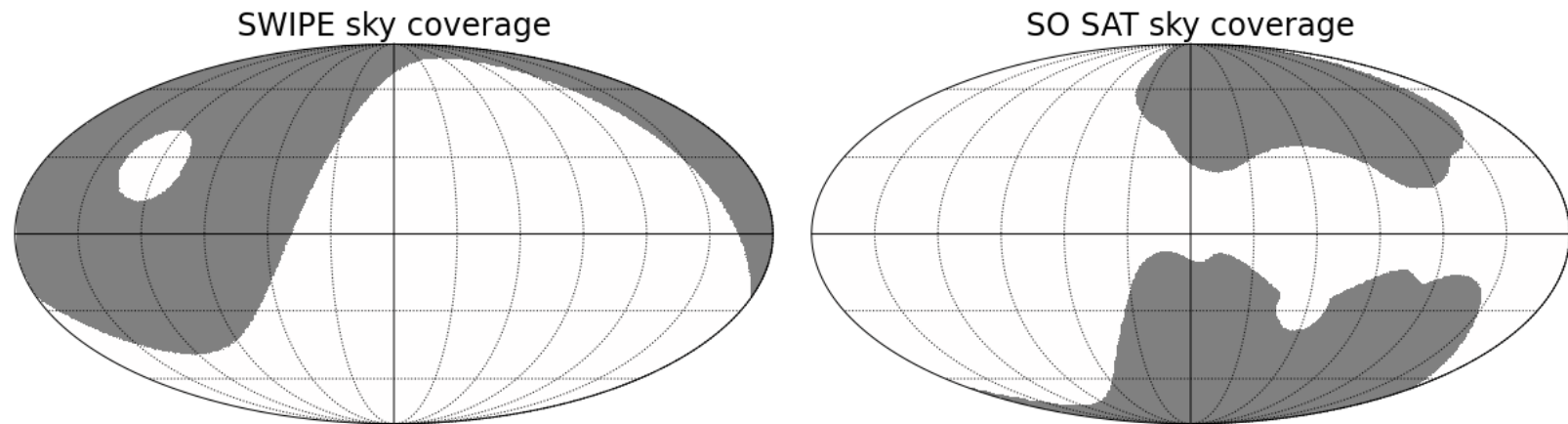
E-B LEAKAGE

$$\tilde{a}_{\pm 2,\ell m} = \int (Q \pm iU) \cdot W(\hat{n}) \cdot Y_{\ell m}^{\pm 2} d\Omega$$

$$\tilde{a}_{\ell m}^E = -\frac{1}{2}(\tilde{a}_{2,\ell m} + \tilde{a}_{-2,\ell m})$$

$$\tilde{a}_{\ell m}^B = -\frac{1}{2i}(\tilde{a}_{2,\ell m} - \tilde{a}_{-2,\ell m})$$

(Lewis et al., 2001)



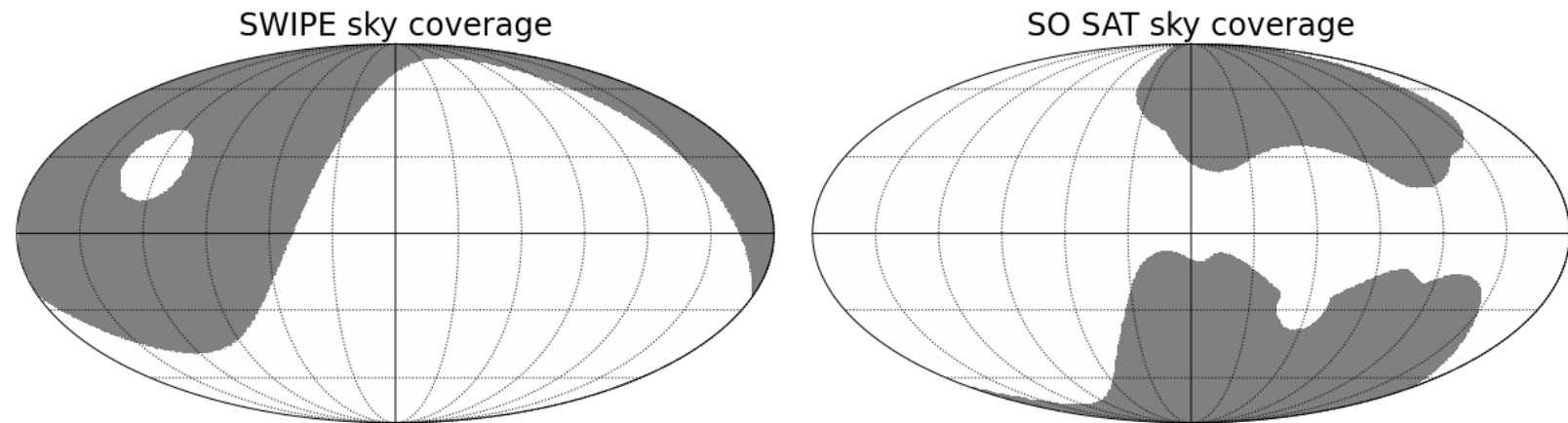
E-B LEAKAGE

$$\tilde{a}_{\pm 2,\ell m} = \int (Q \pm iU) \cdot W(\hat{n}) \cdot Y_{\ell m}^{\pm 2} d\Omega$$

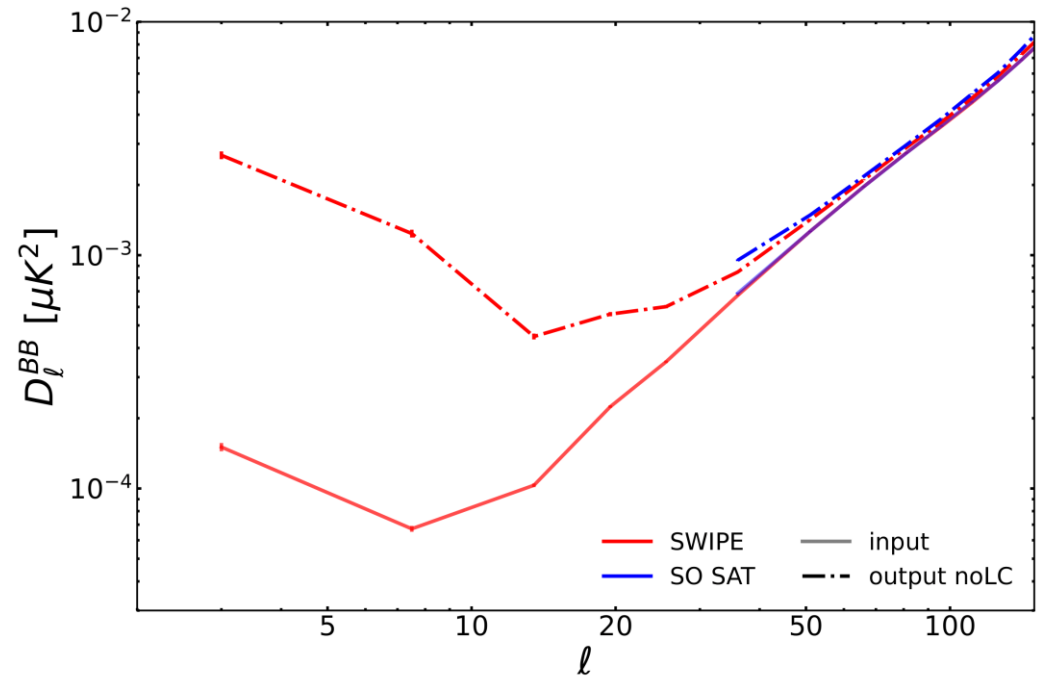
$$\tilde{a}_{\ell m}^E = -\frac{1}{2}(\tilde{a}_{2,\ell m} + \tilde{a}_{-2,\ell m})$$

$$\tilde{a}_{\ell m}^B = -\frac{1}{2i}(\tilde{a}_{2,\ell m} - \tilde{a}_{-2,\ell m})$$

(Lewis et al., 2001)



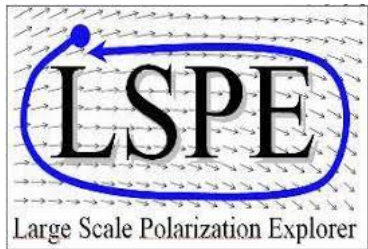
CMB input for all this leakage analysis:
Planck 2018 best-fit parameters + $r = 0.01$



NILC FOR FUTURE B-MODES EXPERIMENTS

Sub-orbital experiments (partial-sky):

Considered experiments:



LSPE-SWIPE (+Planck)

- Balloon-borne
- Target: reionization and recombination bumps with $\delta r=0.015$ (95% CL)
- Frequencies (GHz): 145, 210, 240



Simons Observatory (SO)

- Ground-based
- Target: recombination bump with $\delta r=0.003$ (68% CL)
- Frequencies (GHz): 27, 39, 93, 145, 225, 280

Carones et al. (2023a), arXiv:2208.12059

LEAKAGE CORRECTION (CMB with r=0.01)

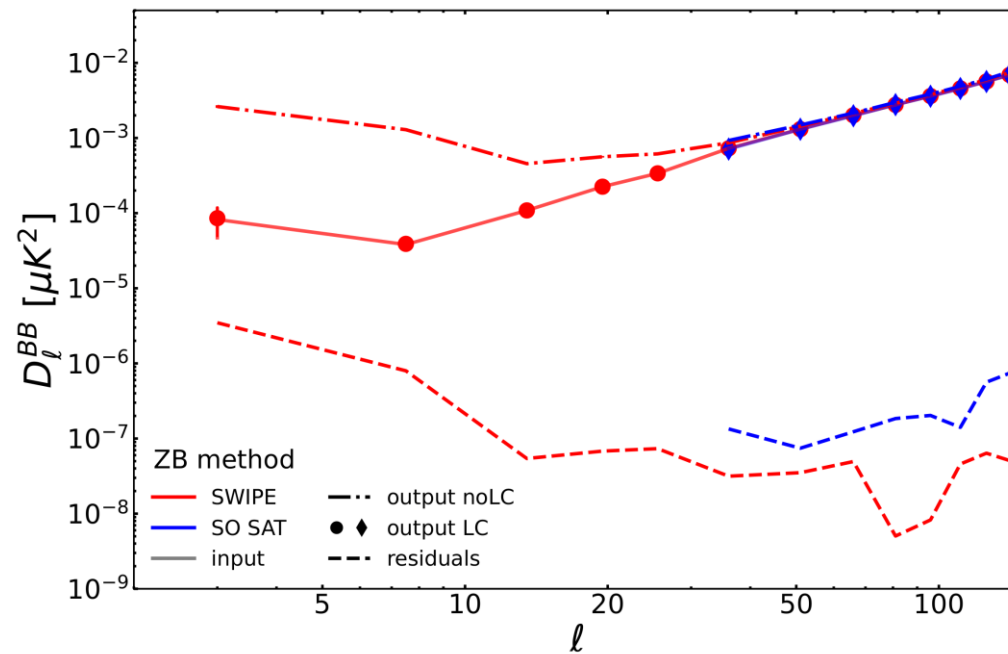
ZB method (Zhao & Baskaran 2010):

$$\mathcal{B}(\hat{\gamma}) = -\frac{1}{2i}[\bar{\delta}_1 \bar{\delta}_2 P_+(\hat{\gamma}) - \delta_1 \delta_2 P_-(\hat{\gamma})]$$

$$\mathcal{B}_{\ell m} = N_\ell B_{\ell m}, \quad N_\ell = \sqrt{(\ell + 2)! / (\ell - 2)!}$$

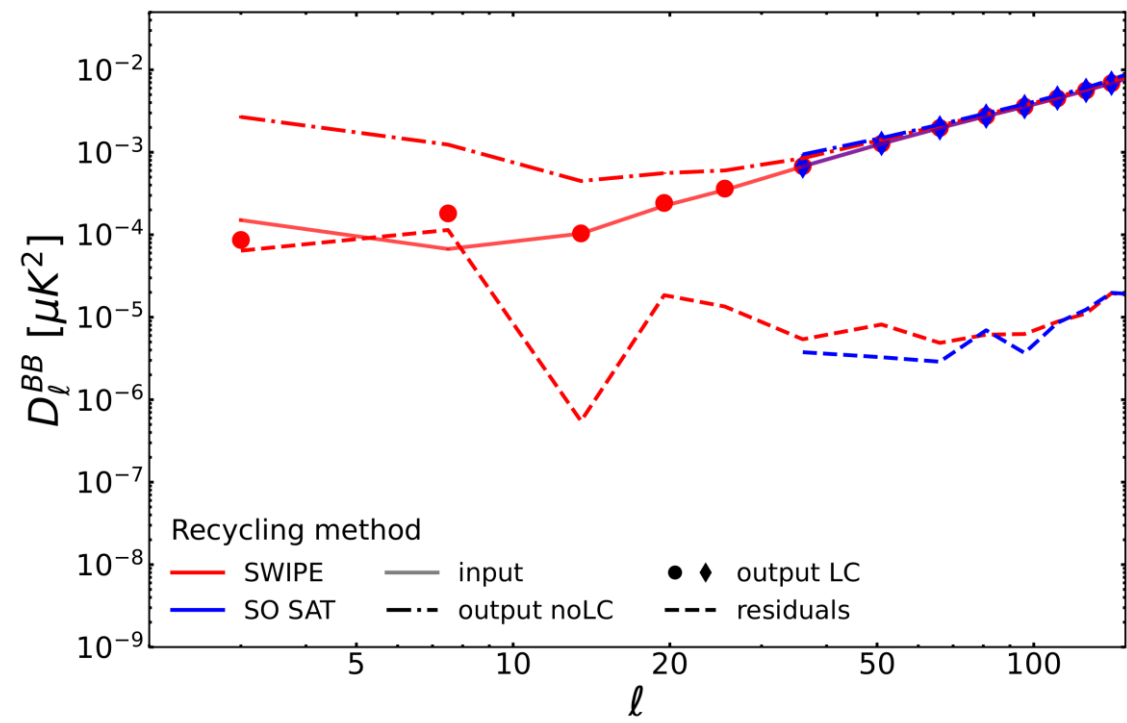
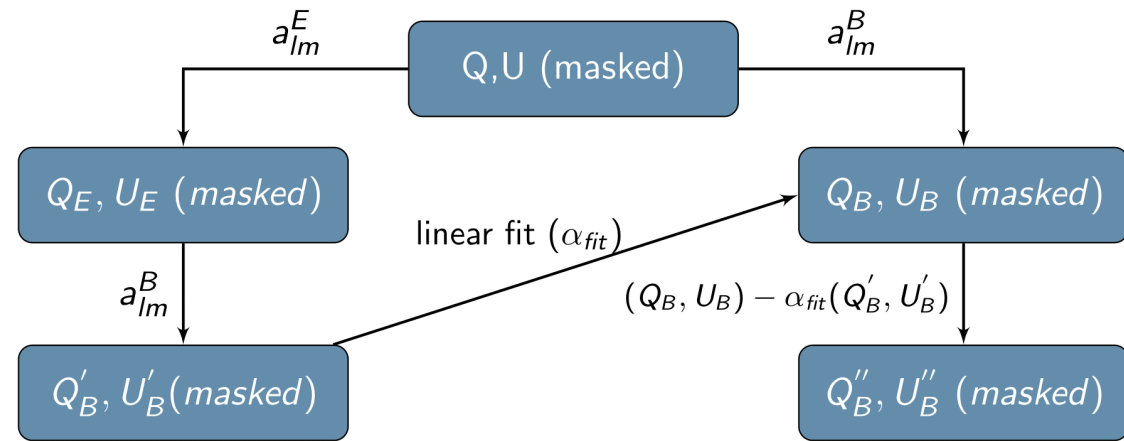
$$\mathcal{B} = \tilde{\mathcal{B}} W^{-1} + ct \cdot W^{-2}$$

$$ct = U[3 \cot \theta WW_x + W(W_{xx} - W_{yy}) - 2(W_x^2 - W_y^2)] \\ - Q[2 \cot \theta WW_y + 2WW_{xy} - 4W_x W_y] \\ - 2W_y[(QW)_x + (UW)_y] + 2W_x[(UW)_x - (QW)_y]$$



LEAKAGE CORRECTION (CMB with $r=0.01$)

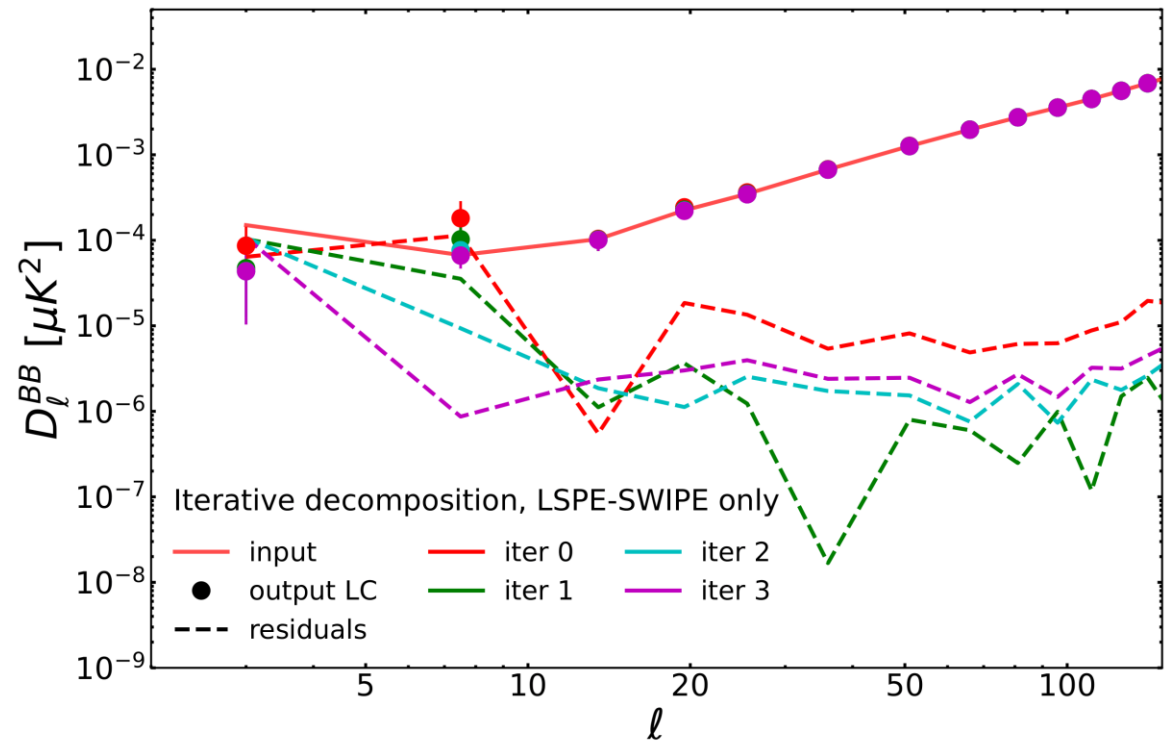
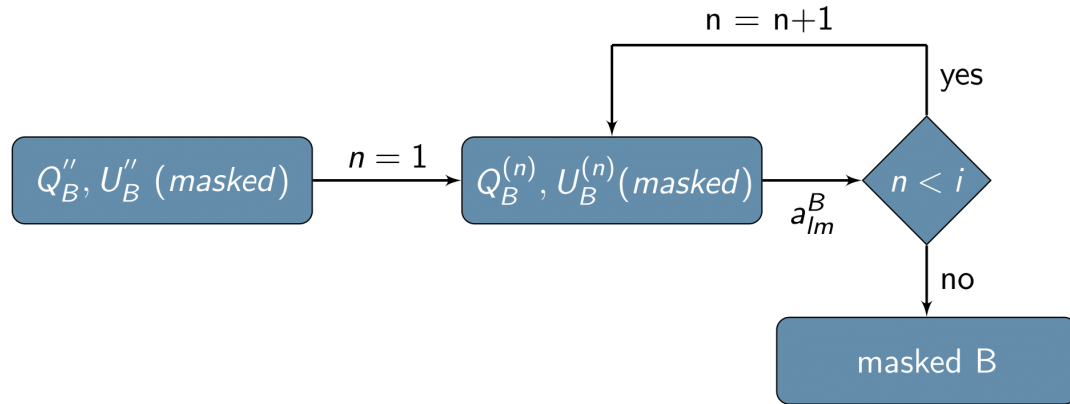
Recycling method (Liu et al. 2019):



E-B LEAKAGE FOR LSPE-SWIPE AT $\ell \lesssim 10$

INNOVATIVE EXTENSIONS FOR LARGE SCALE LEAKAGE CORRECTION

- Iterative B-decomposition:



E-B LEAKAGE FOR LSPE-SWIPE AT $\ell \lesssim 10$

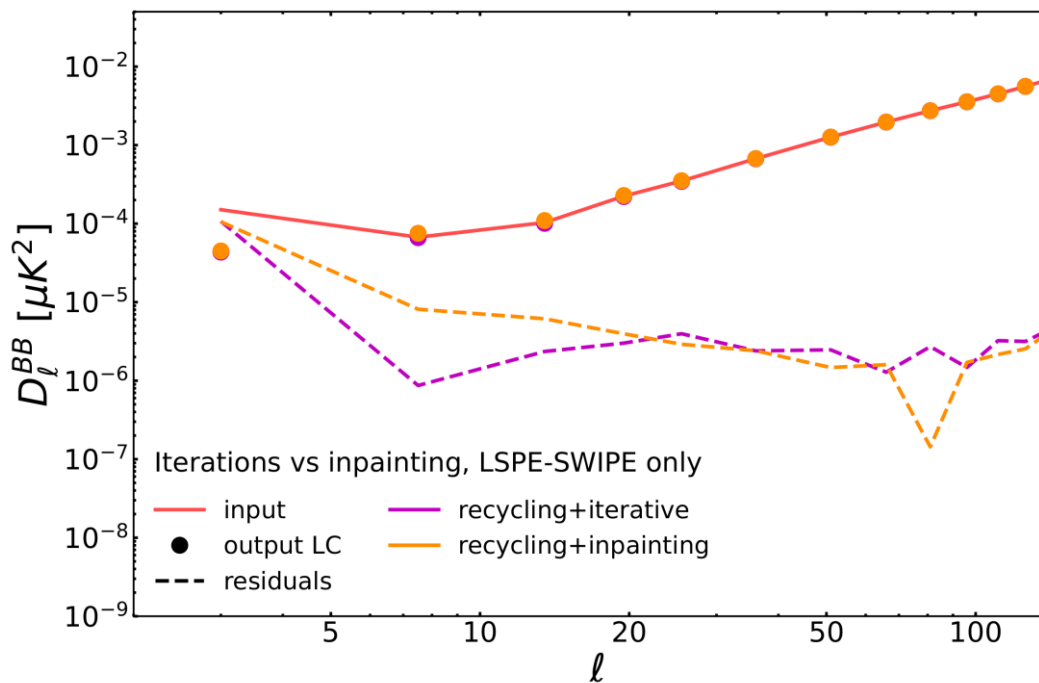
INNOVATIVE EXTENSIONS FOR LARGE SCALE LEAKAGE CORRECTION

- Diffusive inpainting:

Equation for ambiguous modes which cause the E-B leakage:

$$\nabla^2(\nabla^2 + 2)\psi = 0 \quad + \text{Neumann and Dirichlet boundary conditions}$$

The approximate solution is given by the diffusive inpainting



RESULTS (CMB with r=0)

$$-2 \log \mathcal{L}(r) = \sum_{\ell_b, \ell_b^*} (\mathbf{C}_{\ell_b}^{\text{fgds}} - \mathbf{r} \cdot \mathbf{C}_{\ell_b}^{r=1}) \mathbf{M}_{\ell_b \ell_b^*}^{-1} (\mathbf{C}_{\ell_b^*}^{\text{fgds}} - \mathbf{r} \cdot \mathbf{C}_{\ell_b^*}^{r=1})$$

$$\mathbf{M}_{\ell_b \ell_b^*} = \mathbf{Cov}\left(\mathbf{C}_{\ell_b}^{\text{lens}} - (1 - A_L) \cdot \mathbf{C}_{\ell_b}^{\text{lens}}, \mathbf{C}_{\ell_b^*}^{\text{lens}} - (1 - A_L) \cdot \mathbf{C}_{\ell_b^*}^{\text{lens}}\right)$$

$f_{\text{sky}} = 36\%$

$f_{\text{sky}} = 12\%$

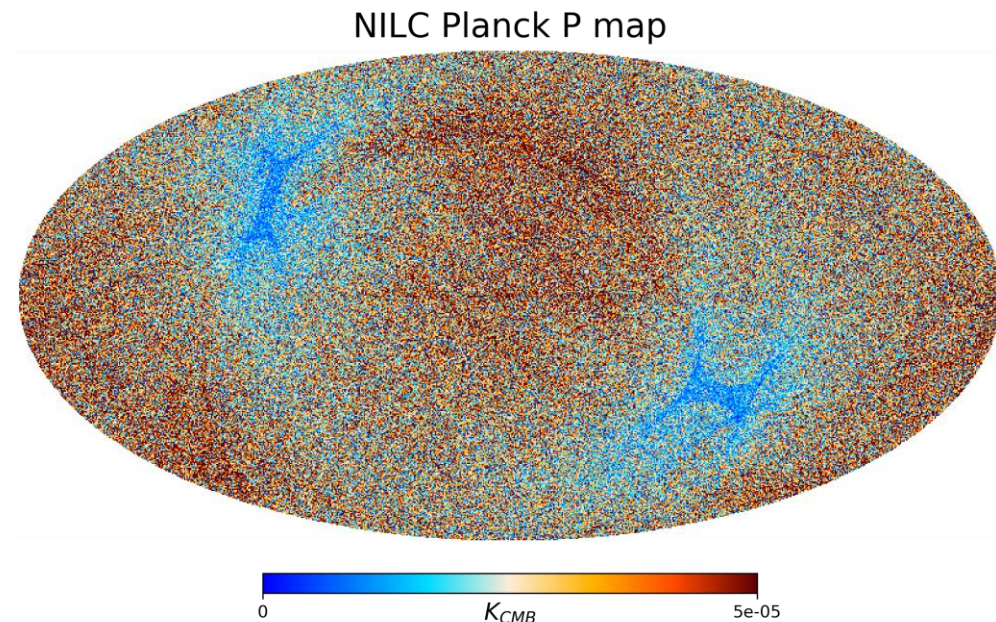
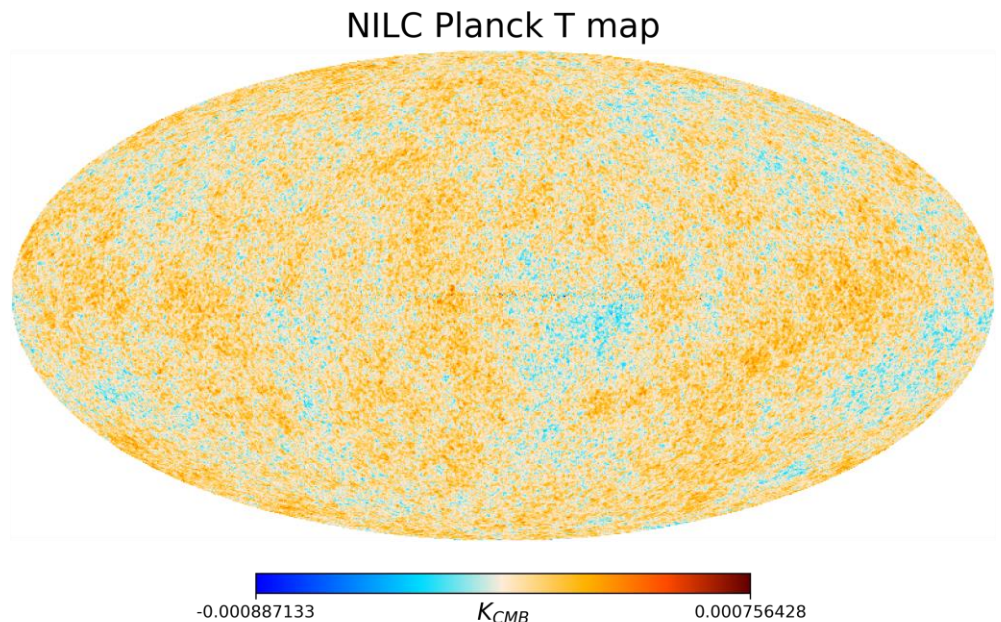
$f_{\text{sky}} = 8\%$

	SWIPE+Planck, d0s0	SWIPE+Planck, d1s1	SO SAT, d1s1
Targets	$r < 0.015$ (95% CL)	$r < 0.015$ (95% CL)	$r < 0.003$ (68% CL)
r-NILC			$r < 0.0027$ (68% CL)
rit-NILC	$r < 0.013$ (95% CL)	$r < 0.024$ (95% CL)	
rin-NILC	$r < 0.015$ (95% CL)	$r < 0.028$ (95% CL)	
HZB-NILC	$r < 0.005$ (95% CL)	$r < 0.015$ (95% CL)	$r < 0.0026$ (68% CL)

NILC FOR PLANCK

- NILC successfully applied to Planck CMB data

(*Planck Collaboration*)



- But:

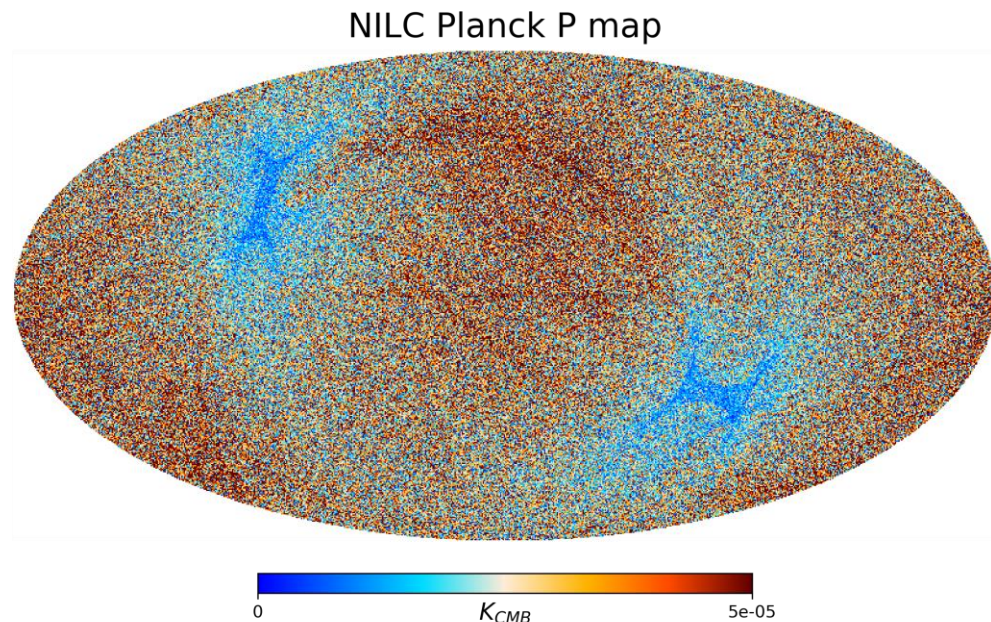
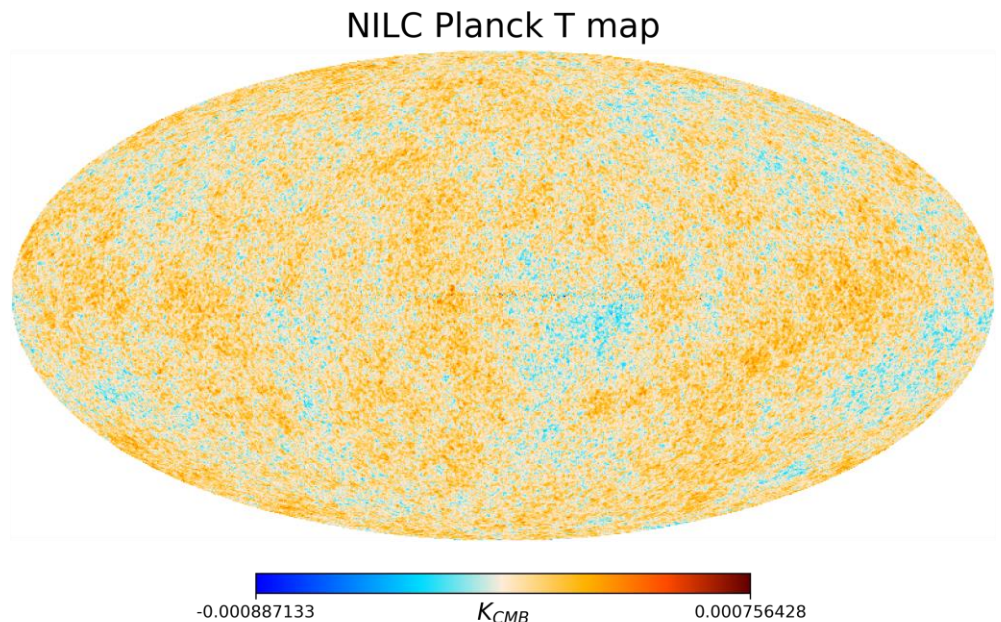
- It cannot be consistently applied to partial-sky polarization data from sub-orbital experiments with its current implementation ✓

Carones et al. (2023a), arXiv:2208.12059

NILC FOR PLANCK

- NILC successfully applied to Planck CMB data

(*Planck Collaboration*)



- But:

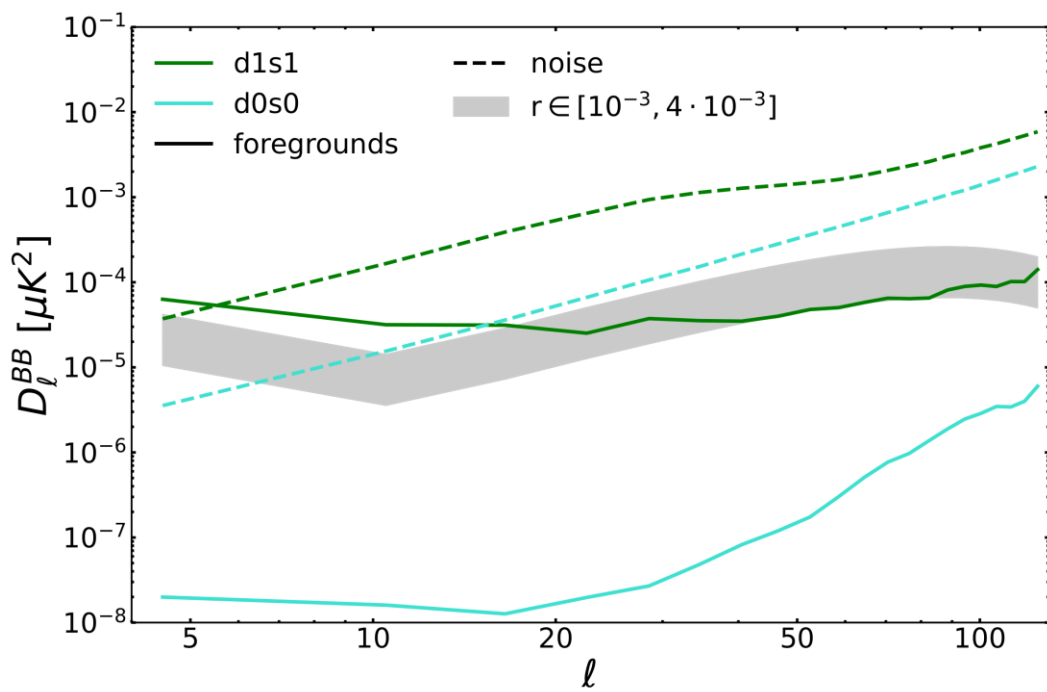
- It cannot be consistently applied to partial-sky polarization data from sub-orbital experiments with its current implementation ✓ Carones et al. (2023a), arXiv:2208.12059
- It suffers high residual foreground contamination when applied to simulated CMB satellite datasets which target accurate measurements of CMB polarization

NILC FOR SATELLITE EXPERIMENTS

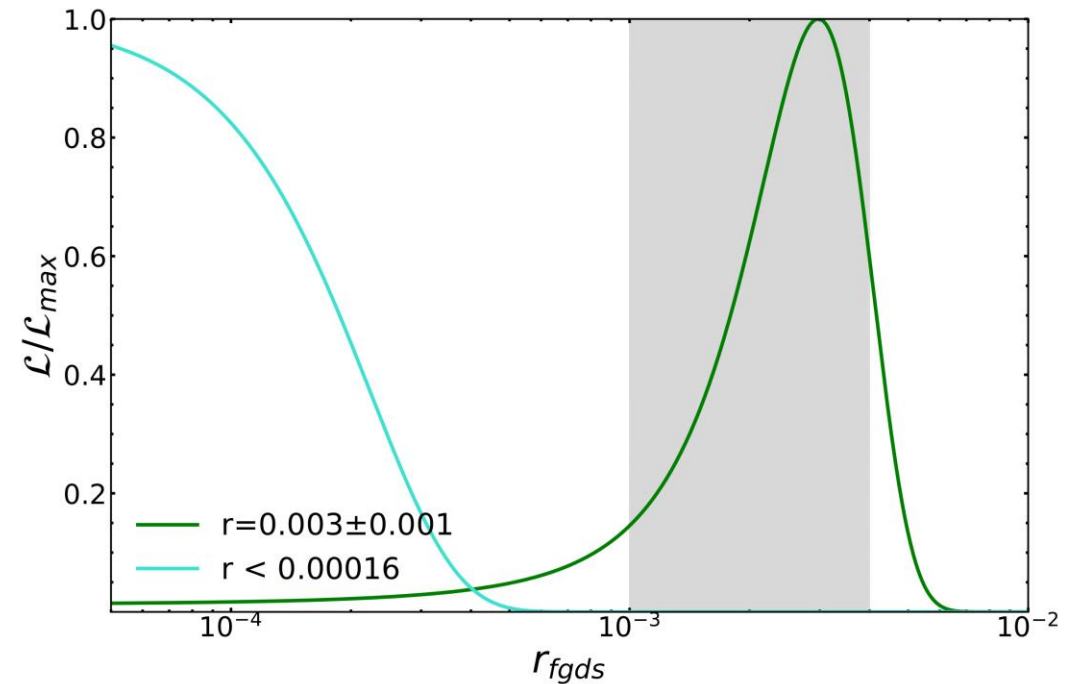
Considered experiment:



LiteBIRD



- Target: reionization and recombination bumps with $\delta r = 0.001$ (68% CL)
- 15 frequency channels (40 – 402 GHz)



Multi-Clustering NILC (MC-NILC)

- Perform independent NILC variance minimization in separate patches of the sky, where B-mode foregrounds present similar properties (SEDs)
- The clusters should be large enough to not introduce a bias in the CMB reconstruction, but small enough to not include too much foregrounds variability

Carones et al. (2023b), arXiv:2212.04456 for the LiteBIRD collaboration

Multi-Clustering NILC (MC-NILC)

- Perform independent NILC variance minimization in separate patches of the sky, where B-mode foregrounds present similar properties (SEDs)
- The clusters should be large enough to not introduce a bias in the CMB reconstruction, but small enough to not include too much foregrounds variability

Carones et al. (2023b), arXiv:2212.04456 for the LiteBIRD collaboration

1. TRACER OF B-MODES FOREGROUNDS SPECTRAL INDICES

Ratio of B-mode Galactic emission templates at two separate frequencies

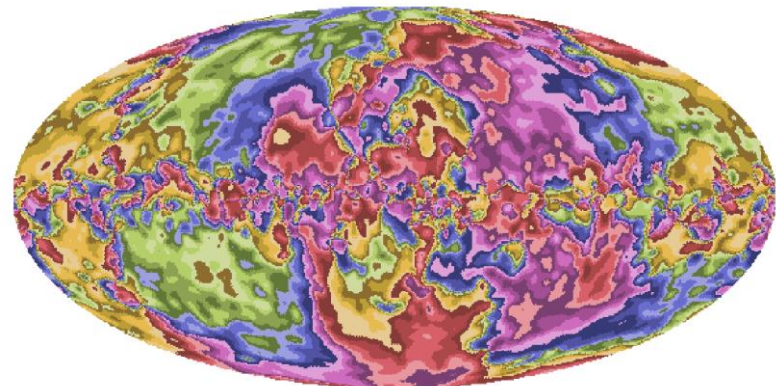
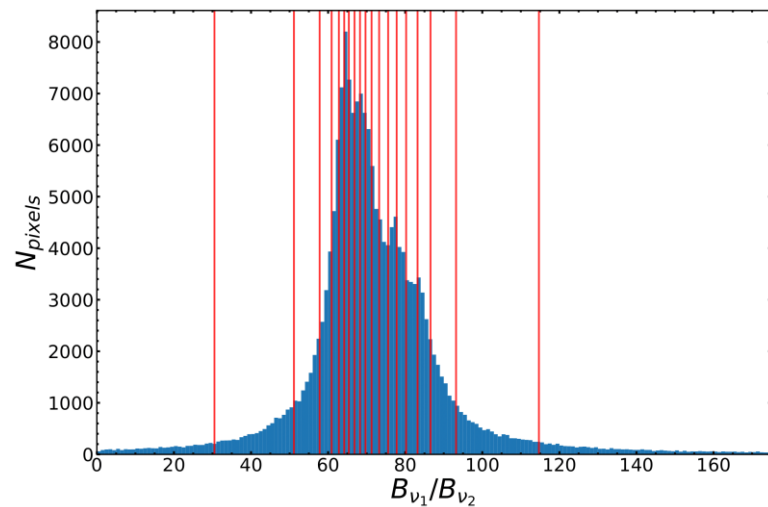
IDEAL CASE: $\frac{\beta_{j, \text{fgds}}^{\nu_1}}{\beta_{j, \text{fgds}}^{\nu_2}}$ input foregrounds-only maps

REALISTIC CASE: $\frac{\beta_{j=0, \text{GNILC}}^{\nu_1}}{\beta_{j=0, \text{GNILC}}^{\nu_2}}$ templates of foreground B-modes from input data

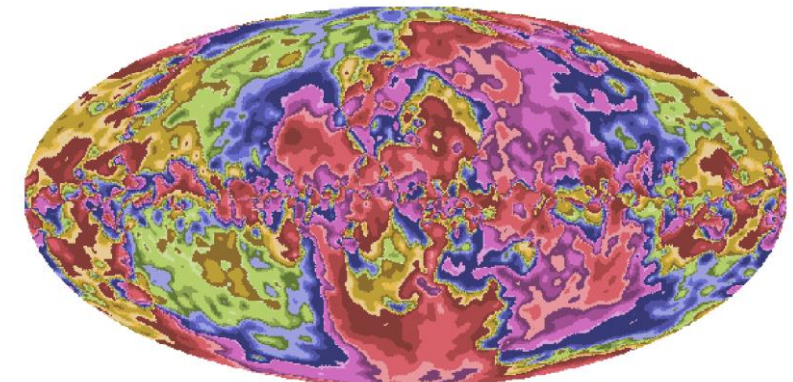
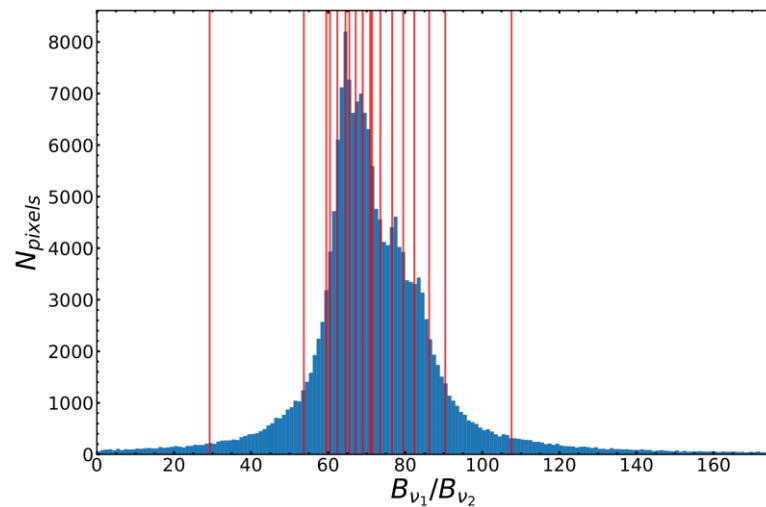
For LiteBIRD, $\nu_1 = 337$ GHz and $\nu_2 = 119$ GHz

2. CLUSTERING TECHNIQUES

Clusters of Equal Area (CEA)

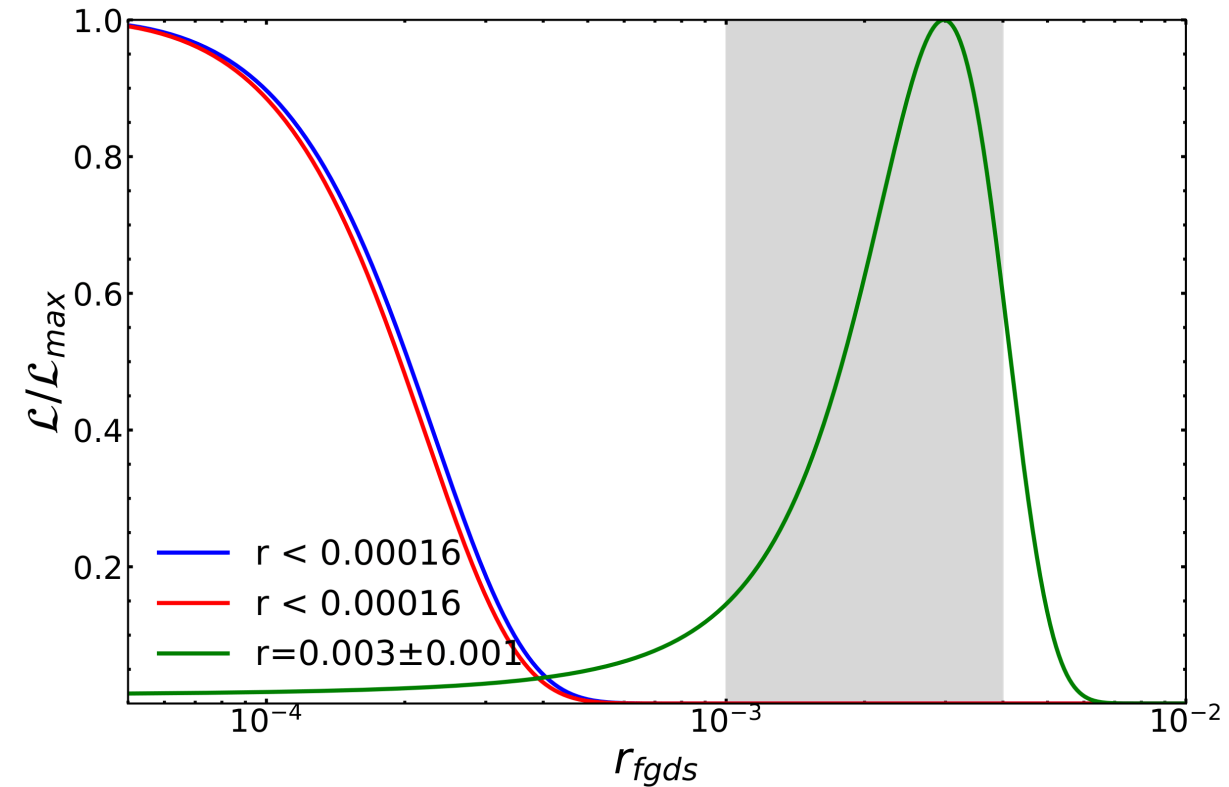
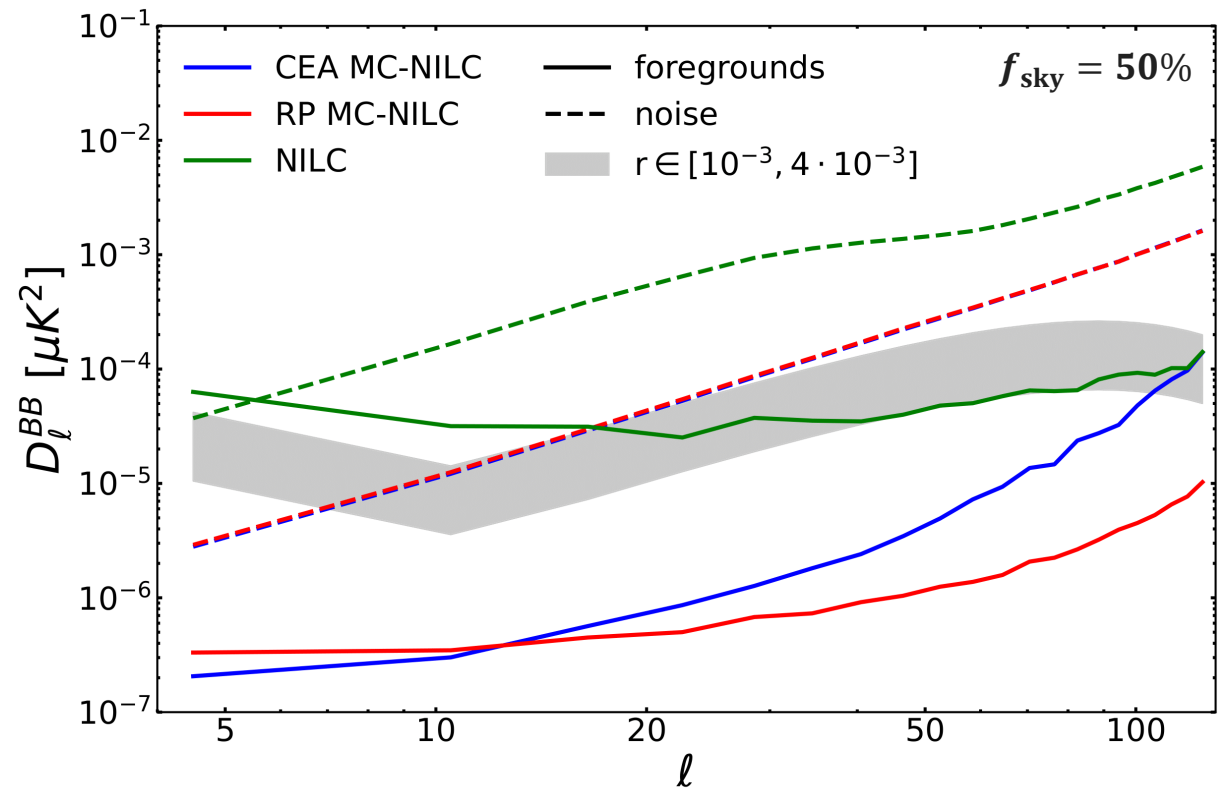


Random Partitions (RP)



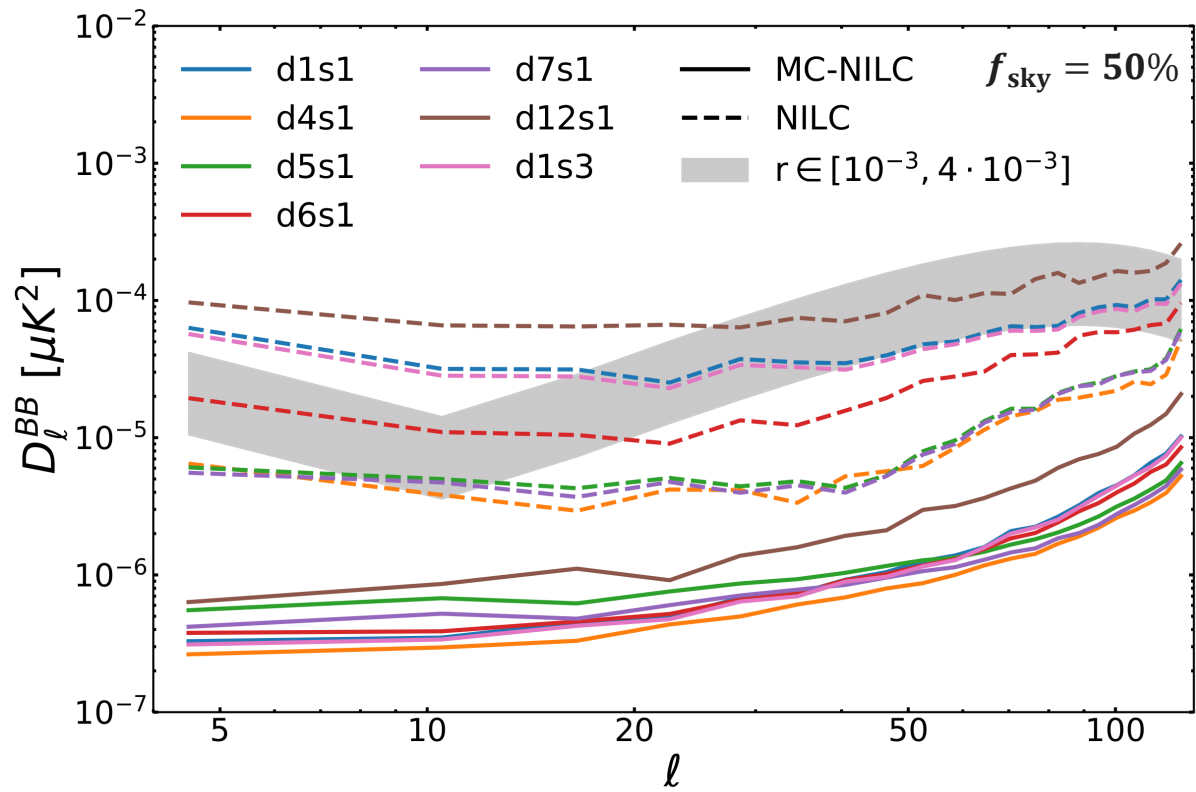
MC-NILC (IDEAL CASE)

- IDEAL CASE:
RATIO BUILT WITH MAPS OF B-MODES SIMULATED FOREGROUNDS AT EACH NEEDLET SCALE

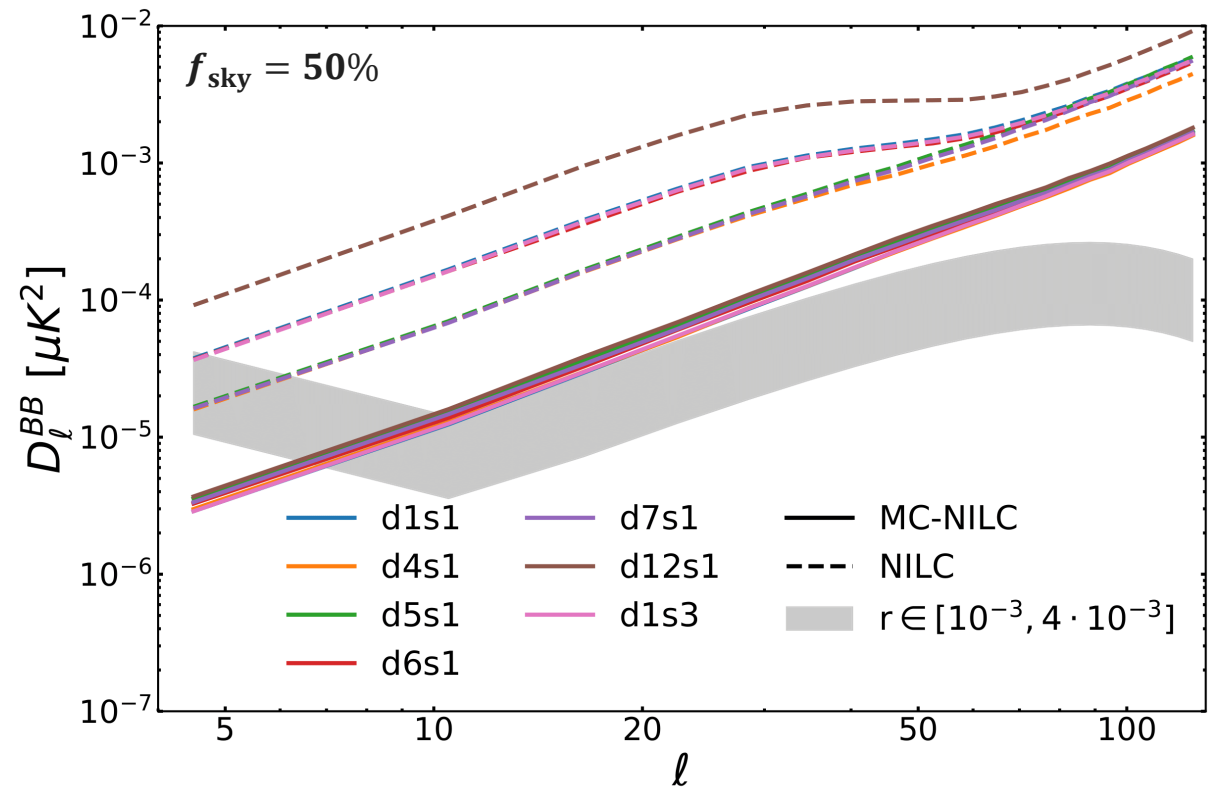


ROBUSTNESS TEST

Foregrounds residuals

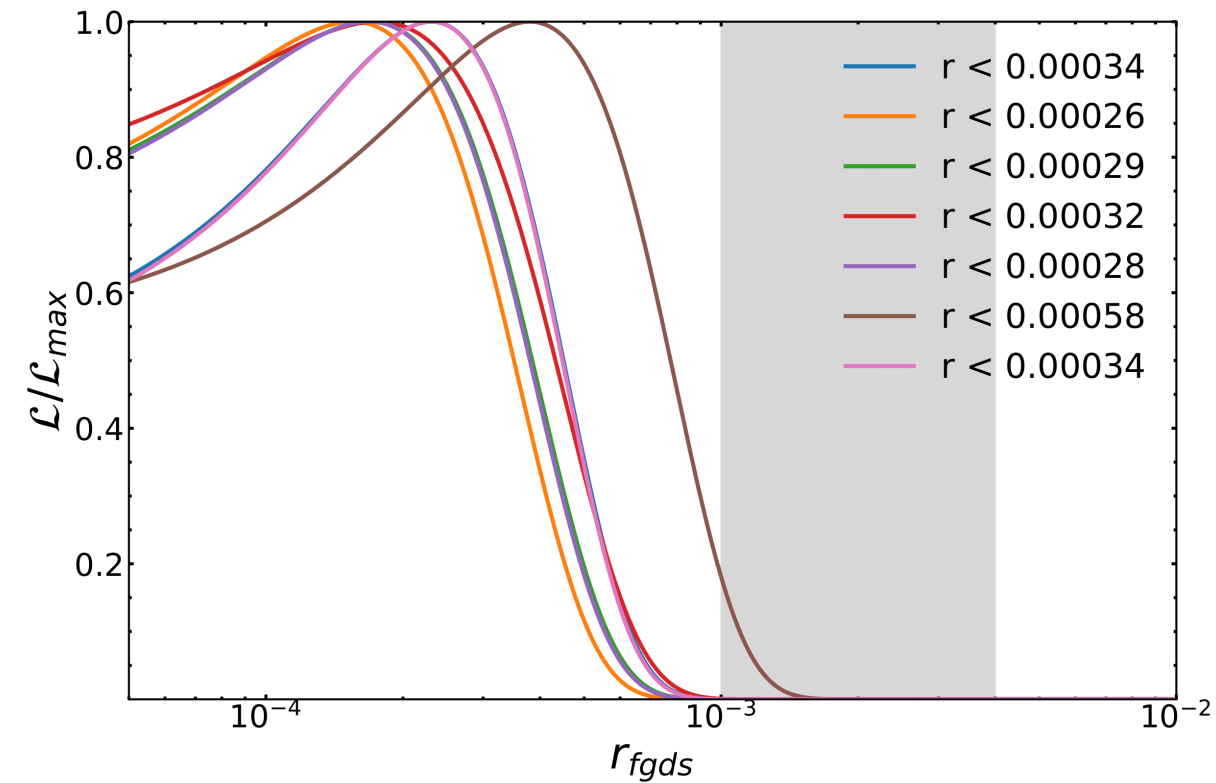
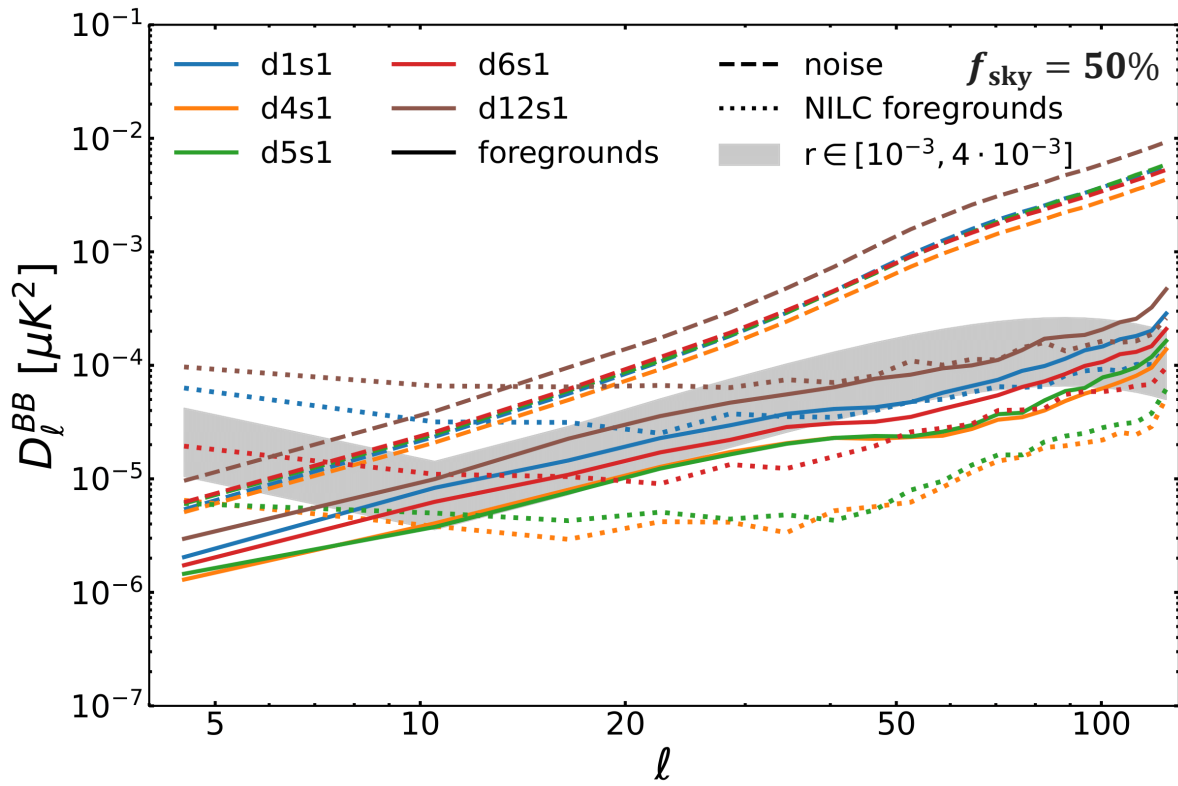


Noise residuals



MC-NILC (REALISTIC CASE)

- REALISTIC CASE:
RATIO BUILT WITH THE Generalized NILC (GNILC, Remazeilles et al., 2011) TEMPLATES OF B-MODES FOREGROUNDS AT FIRST NEEDLET SCALE



CONCLUSIONS

1. Polarized foregrounds will make the detection of primordial CMB B-modes challenging
2. Mis-modeling of their emission can lead to significant biases on the tensor-to-scalar ratio
3. NILC is a powerful blind algorithm, complementary to parametric methods

For sub-orbital CMB experiments devoted to B-modes studies:

- We have to account for the E-B leakage, needlet filtering and beam convolution;
- NILC leads to a level of foregrounds residuals which in most cases would not bias an estimation of the tensor-to-scalar ratio.

(Carones et al. (2023a), arXiv:2208.12059)

For satellite experiments:

- a new foregrounds subtraction algorithm, Multi-Clustering NILC (MC-NILC), is presented;
- MC-NILC performs an independent variance minimization of the output map on different needlet scales and different patches on the sky which trace the spatial variability of spectral properties of B-modes foregrounds;
- MC-NILC lowers simultaneously the foregrounds and noise residuals with respect to NILC when applied to LiteBIRD simulated data permitting to reach the scientific target of the mission.

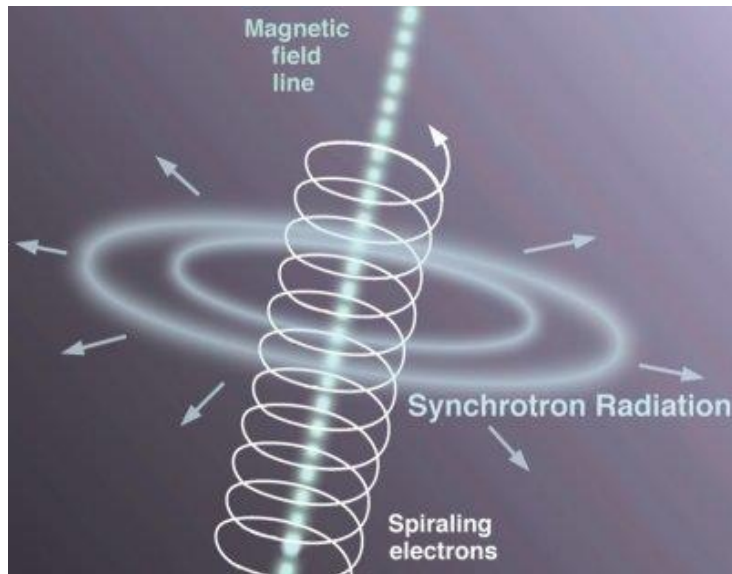
(Carones et al. (2023b), arXiv:2212.04456)

**Thank you
for your attention**

Back-up slides

GALACTIC FOREGROUNDS

- **Synchrotron:**

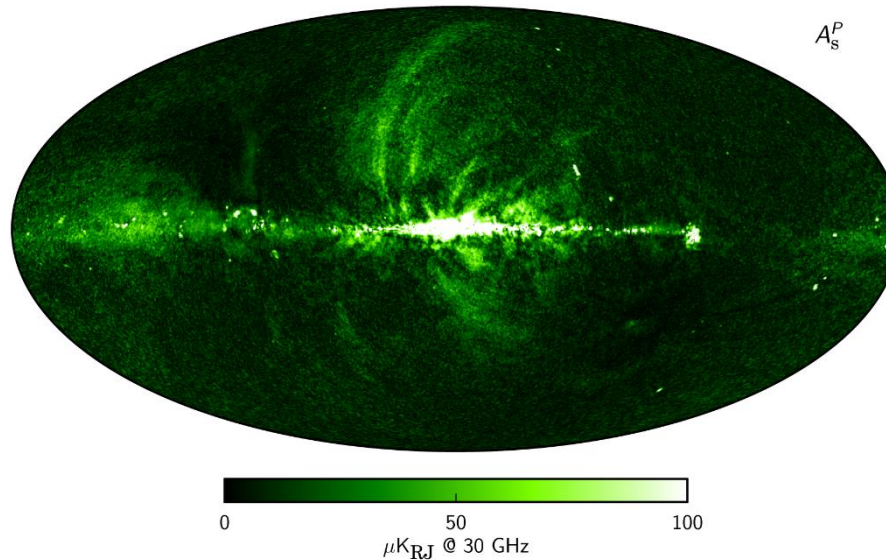


$$X_s(\nu, p) = A_s(p) \cdot \left(\frac{\nu}{\nu_s}\right)^{\beta_s(p)}$$

$$X = \{I, Q, U\}$$

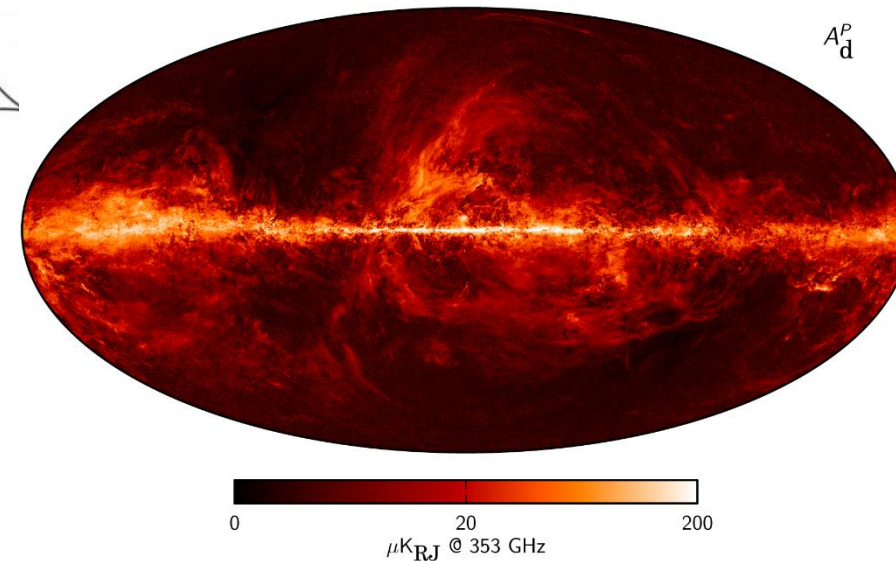
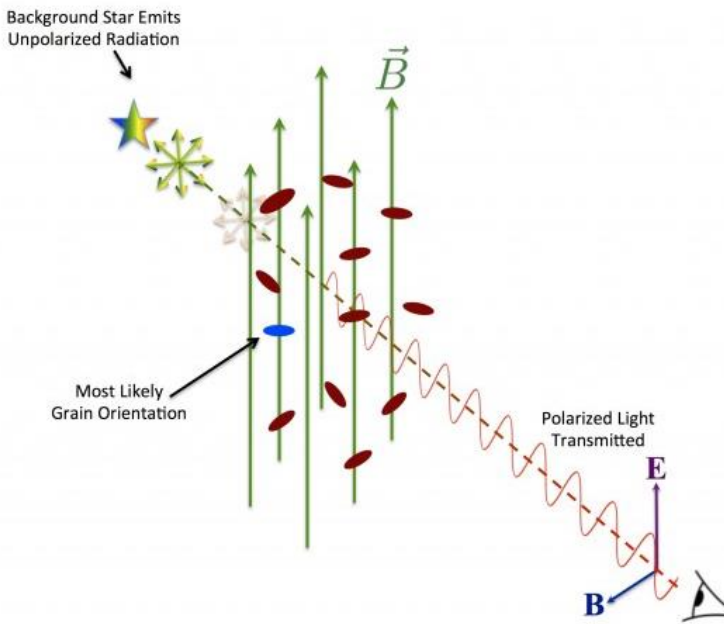
Popular models in PySM (Zonca et al., 2021):

- **s0: constant spectral index**
- **s1: anisotropic spectral index across the sky**



GALACTIC FOREGROUNDS

- Thermal dust:



$$X_d(\nu, p) = A_d(p) \cdot \left(\frac{\nu}{\nu_d} \right)^{\beta_d(p)+1} \frac{B(\nu, T_d(p))}{B(\nu_d, T_d(p))}$$

$$X = \{I, Q, U\}$$

Popular models in PySM (Zonca et al., 2021):

- **$d0$: constant spectral parameters**
- **$d1$: anisotropic spectral parameters across the sky**

... but many others still
in agreement with Planck data

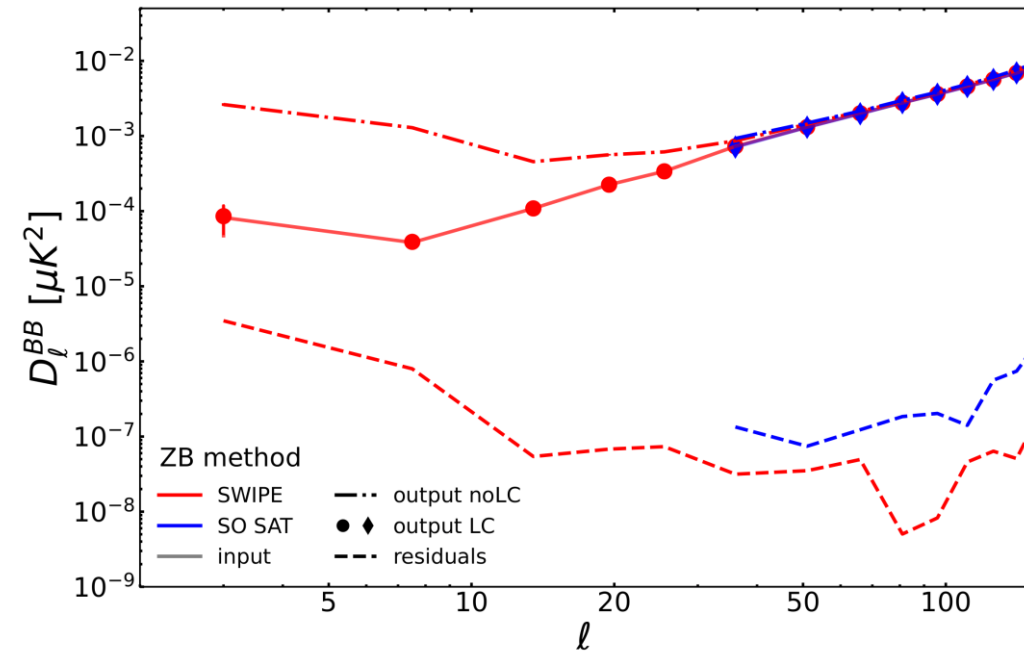
LEAKAGE CORRECTION (CMB with $r=0.01$)

ZB method (Zhao & Baskaran 2010):

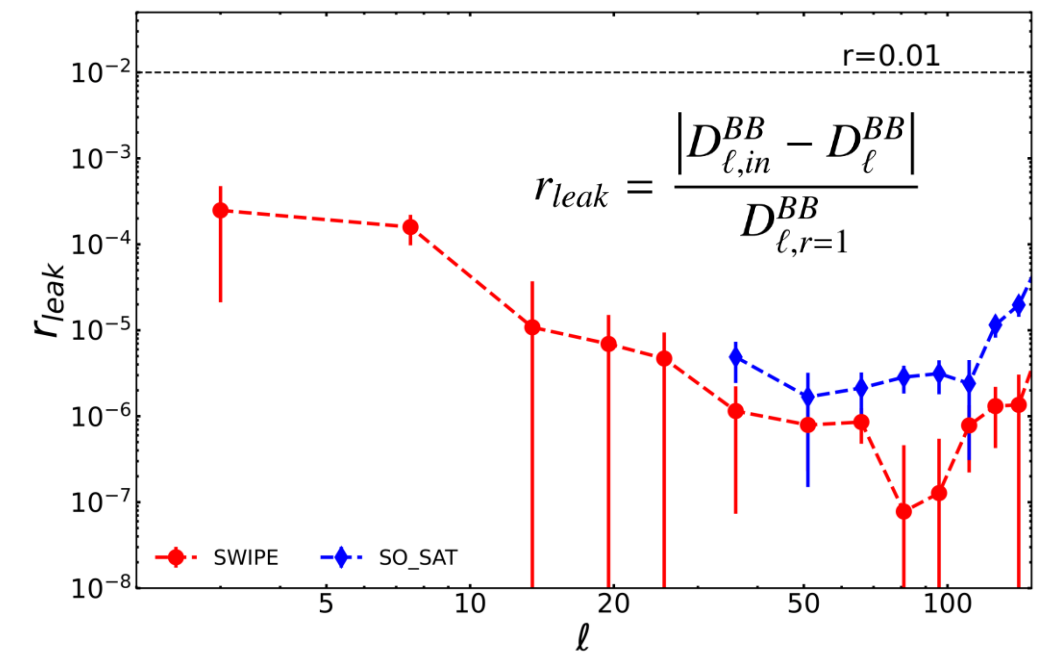
$$\mathcal{B}(\hat{\gamma}) = -\frac{1}{2i}[\bar{\delta}_1 \bar{\delta}_2 P_+(\hat{\gamma}) - \bar{\delta}_1 \bar{\delta}_2 P_-(\hat{\gamma})]$$

$$\mathcal{B}_{\ell m} = N_\ell B_{\ell m}, \quad N_\ell = \sqrt{(\ell + 2)! / (\ell - 2)!}$$

$$\mathcal{B} = \tilde{\mathcal{B}} W^{-1} + ct \cdot W^{-2}$$

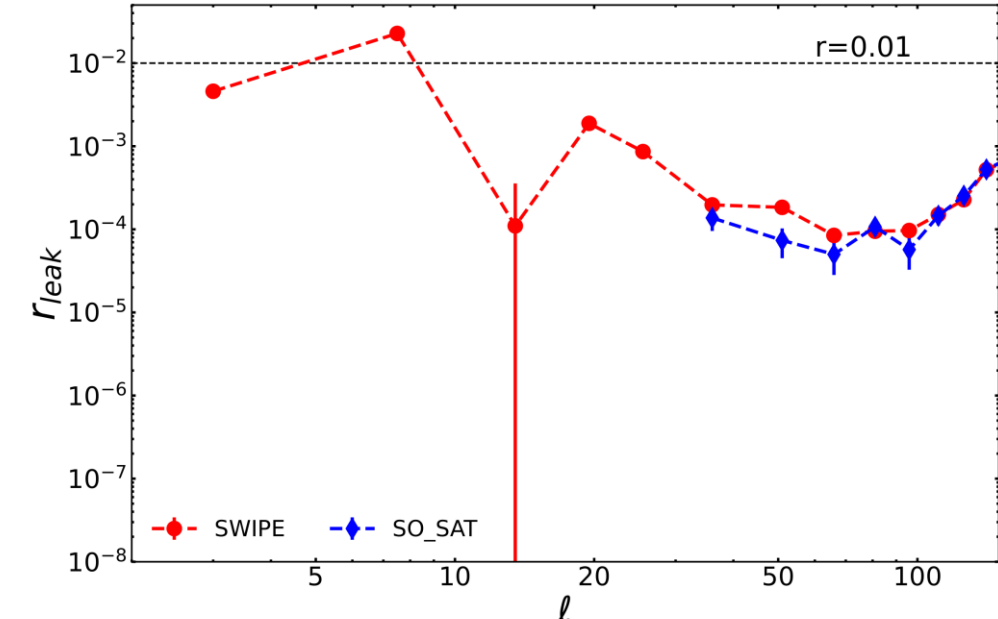
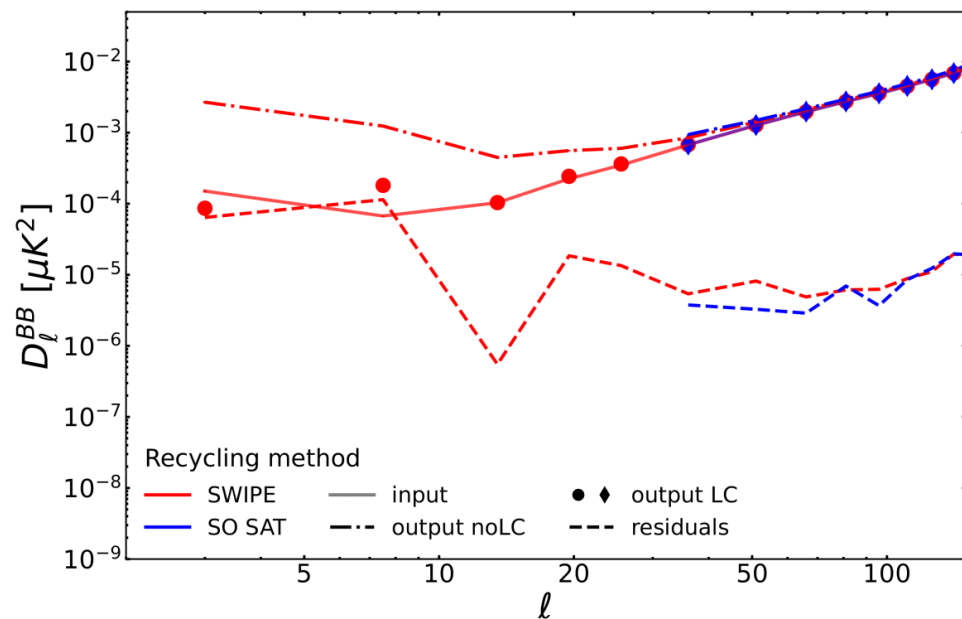
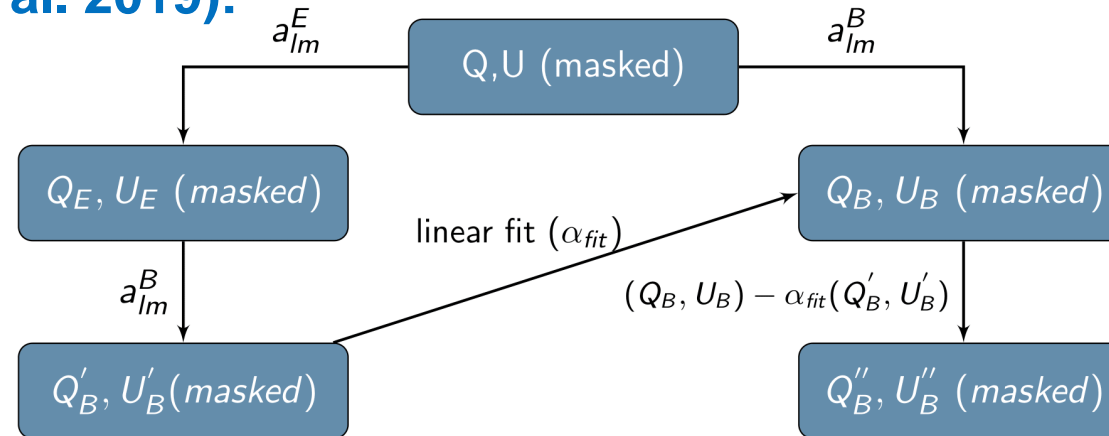


$$ct = U[3 \cot \theta WW_x + W(W_{xx} - W_{yy}) - 2(W_x^2 - W_y^2)] \\ - Q[2 \cot \theta WW_y + 2WW_{xy} - 4W_x W_y] \\ - 2W_y[(QW)_x + (UW)_y] + 2W_x[(UW)_x - (QW)_y]$$



LEAKAGE CORRECTION (CMB with $r=0.01$)

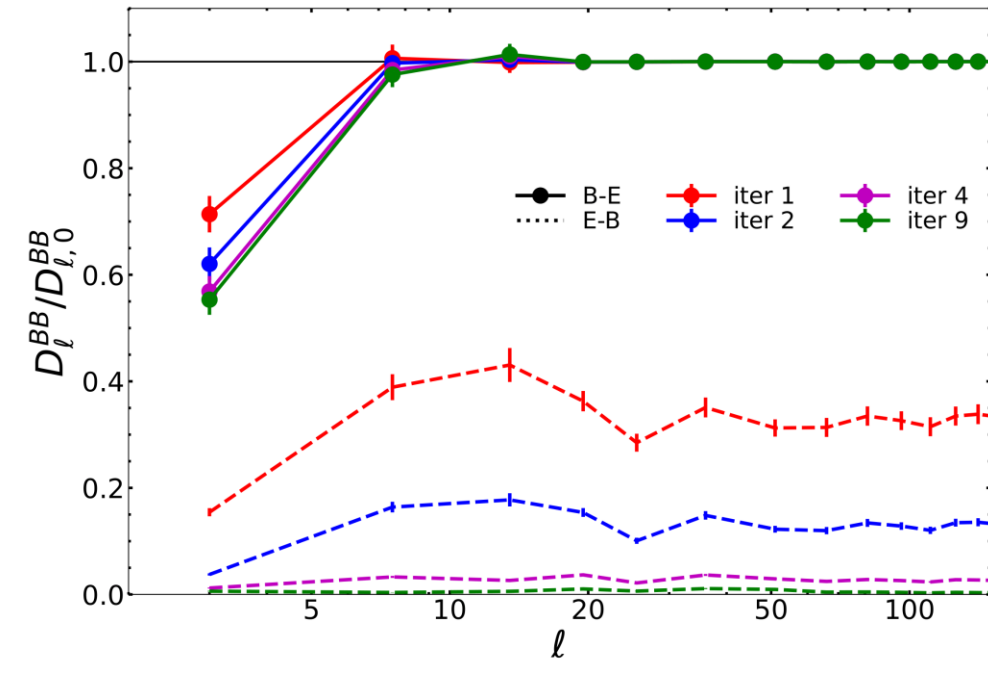
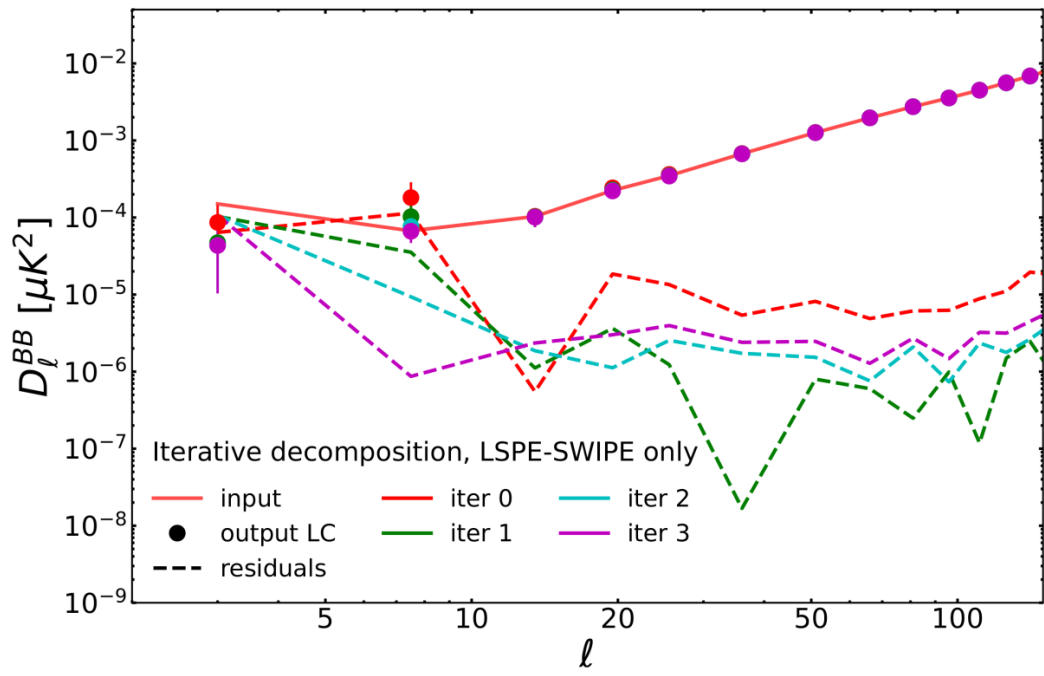
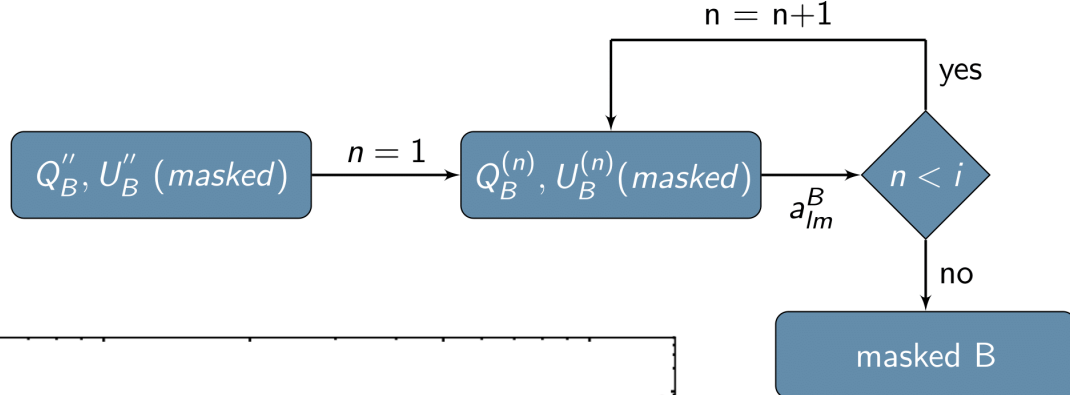
Recycling method (Liu et al. 2019):



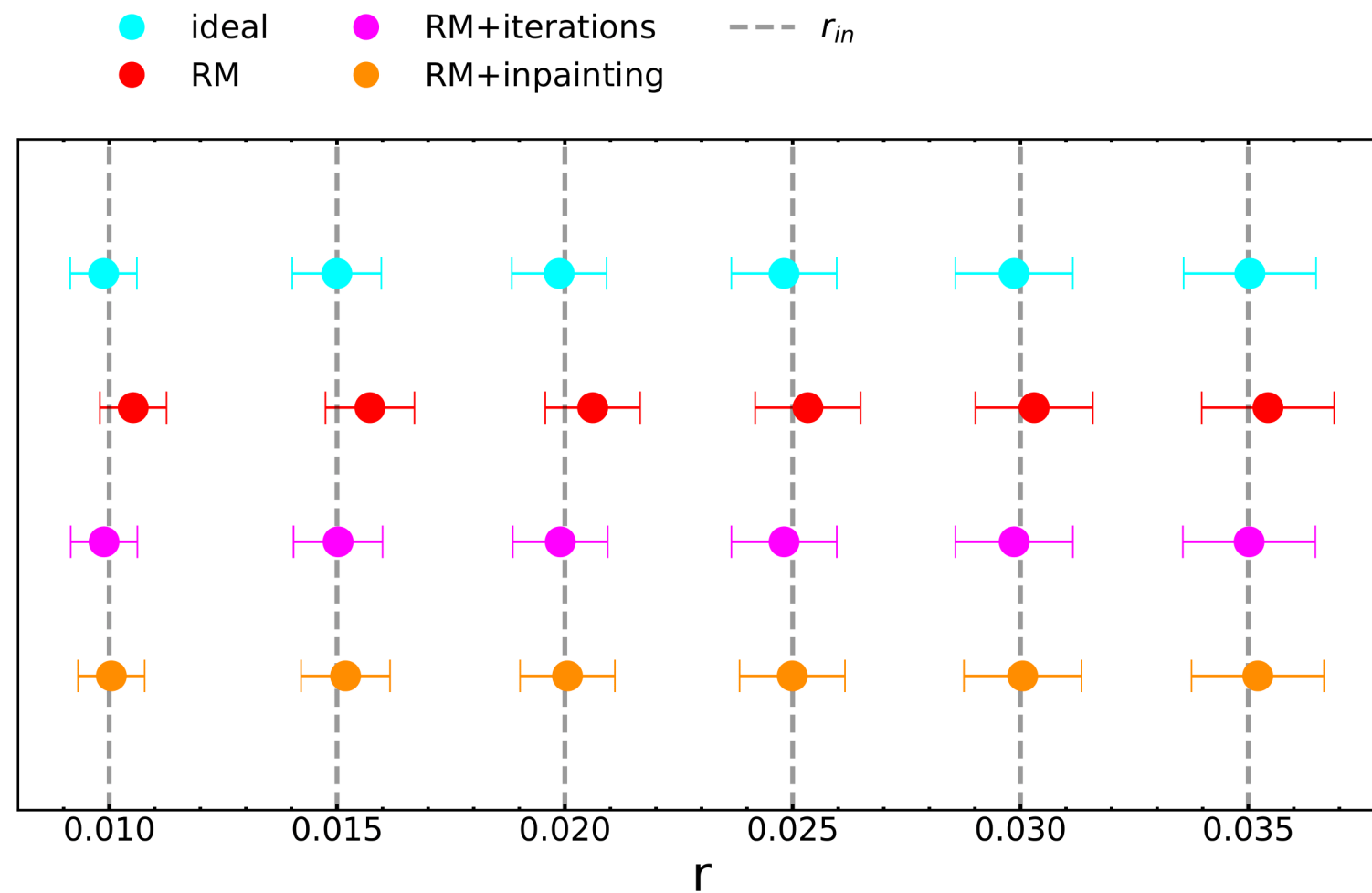
E-B LEAKAGE FOR LSPE-SWIPE AT $\ell \lesssim 10$

INNOVATIVE EXTENSIONS FOR LARGE SCALE LEAKAGE CORRECTION

- Iterative B-decomposition:

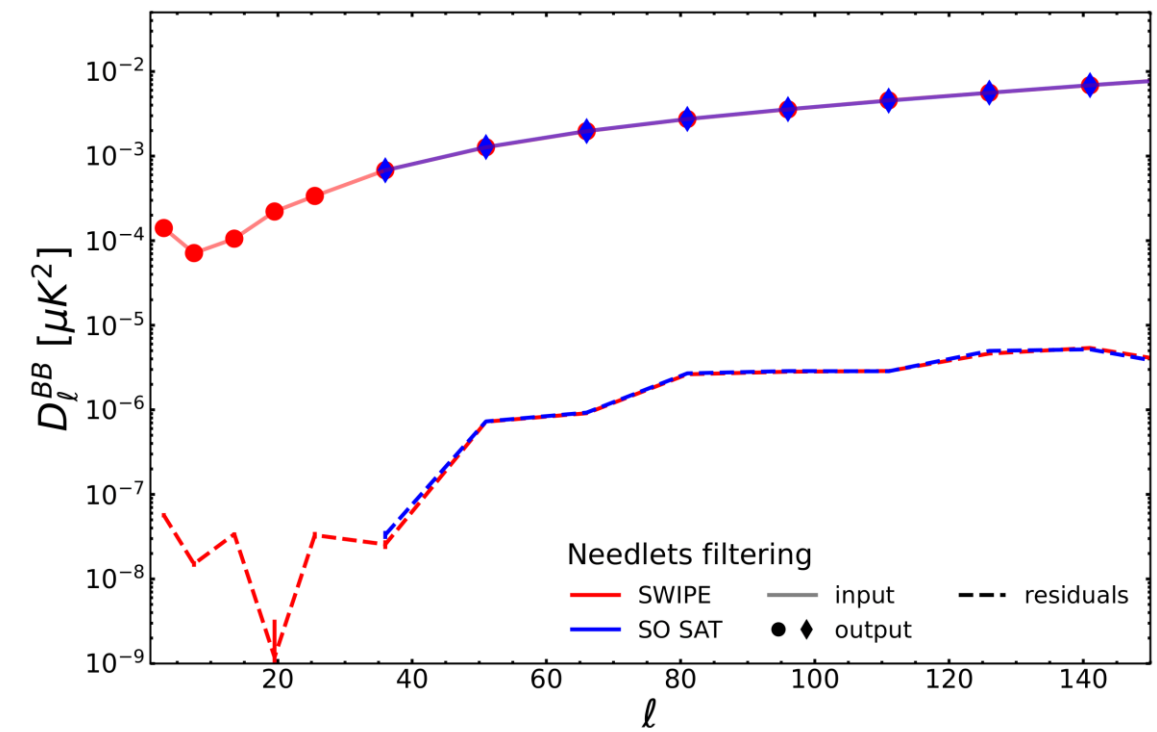


LEAKAGE CORRECTION

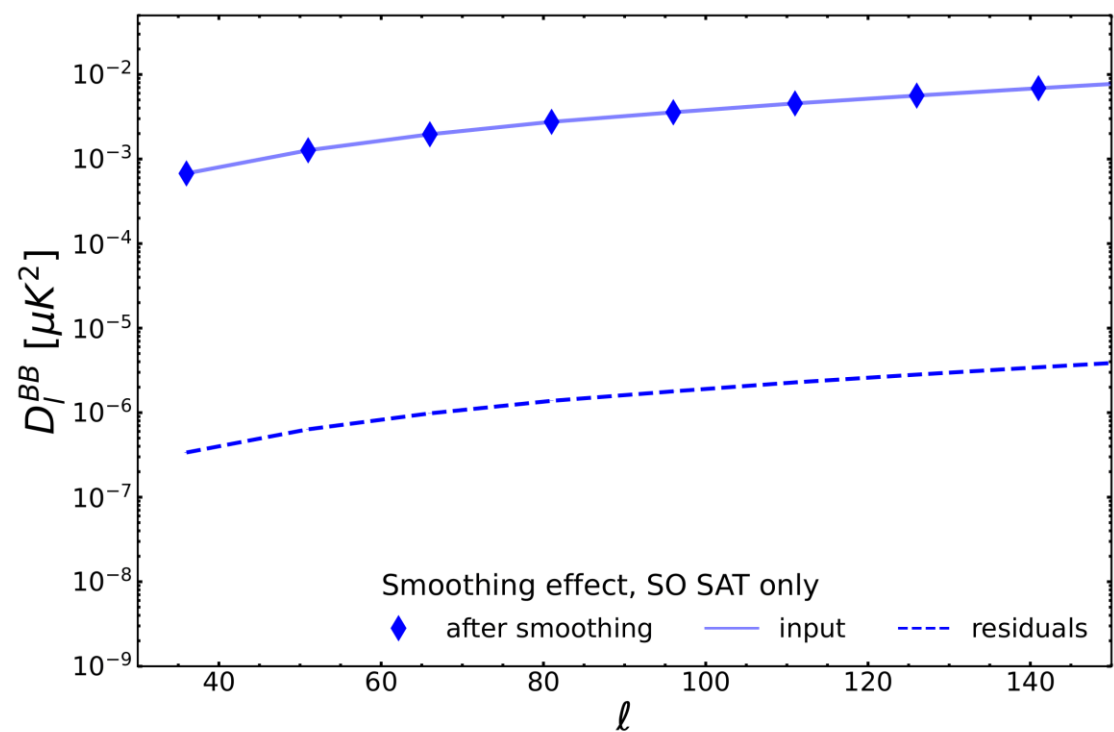


CONVOLUTIONS (CMB with r=0.01)

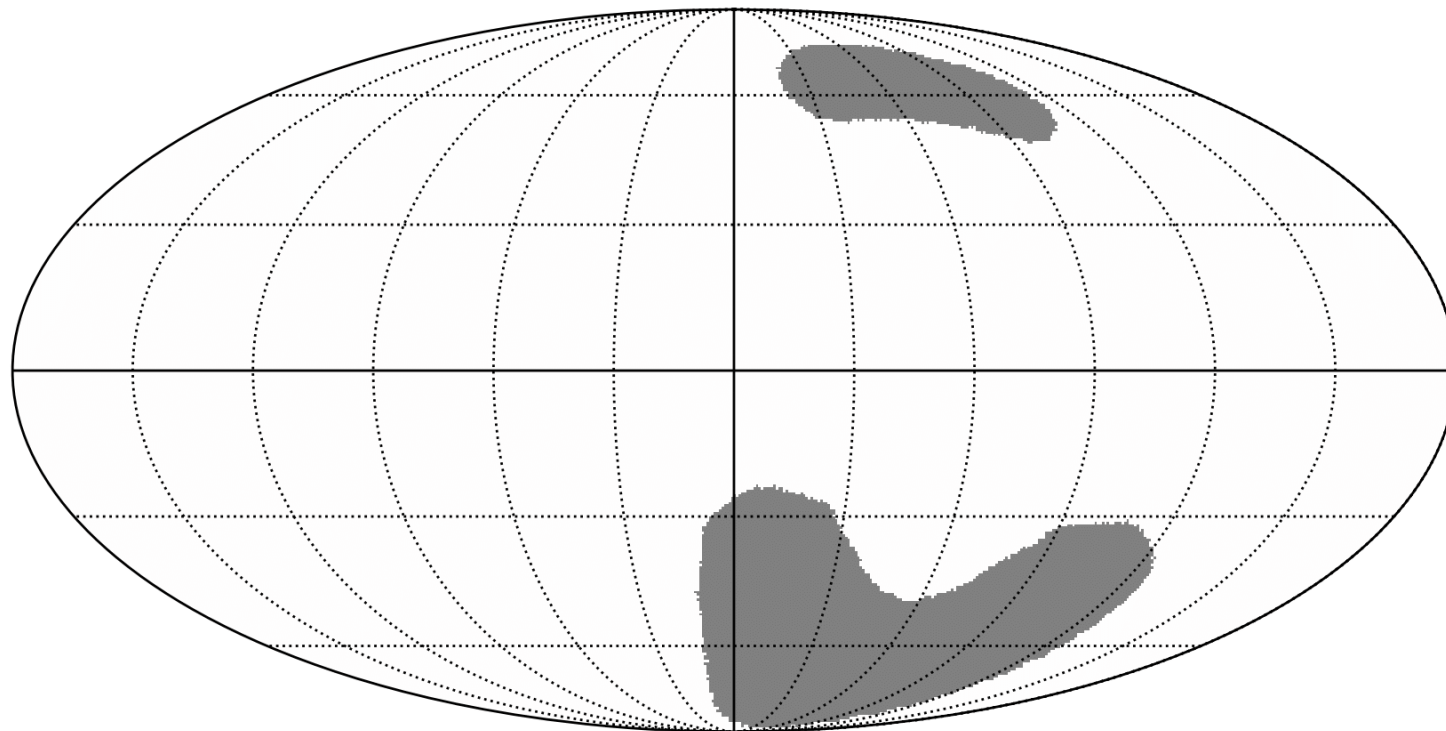
Needlet filtering:



Smoothing:



SO PATCH FOR NILC



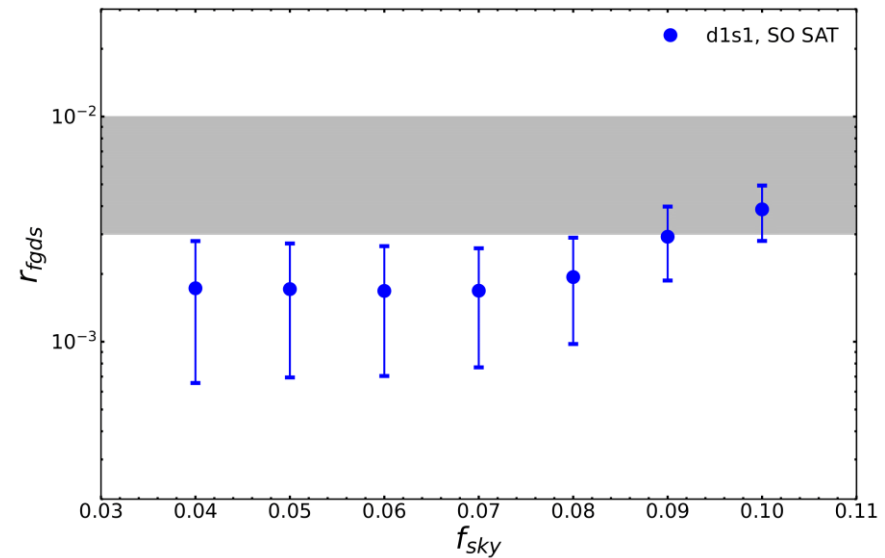
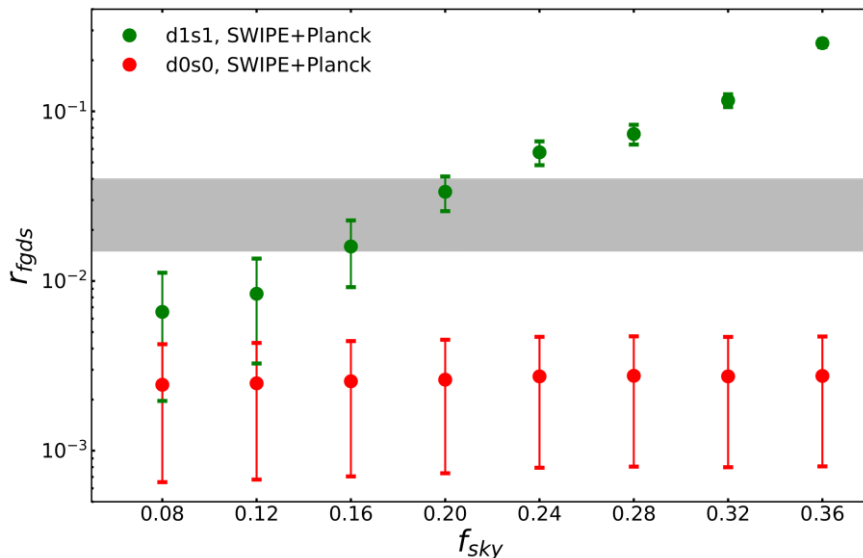
APPLICATION OF NILC

- We have verified that needlet filtering and beam convolutions do not affect the CMB reconstruction
- We are ready to apply NILC on leakage corrected B-modes multi-frequency data:
 - r-NILC: recycling method
 - rit-NILC: recycling + iterative decomposition method
 - rin-NILC: recycling + inpainting method
 - HZB-NILC: ZB method

$$C_{\ell b}^{\text{out}} = \cancel{C_{\ell b}^{\text{lens}}} + C_{\ell b}^{\text{fgds}} + \cancel{C_{\ell b}^{\text{noi}}}$$

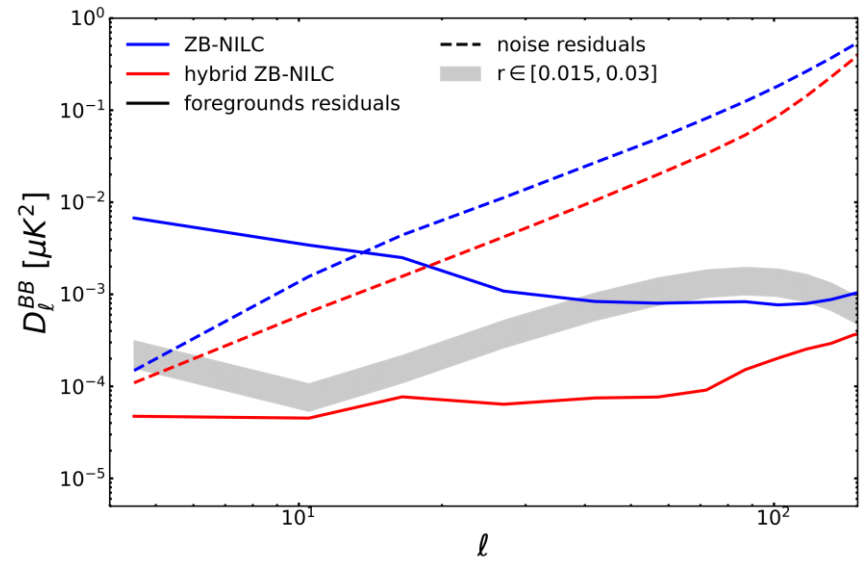
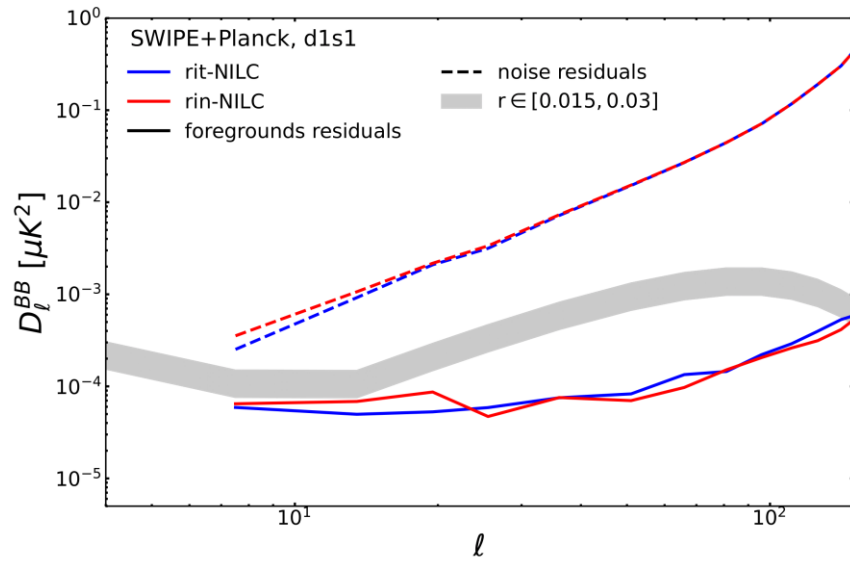
APPLICATION OF NILC

Masking:



No ZB but HZB:

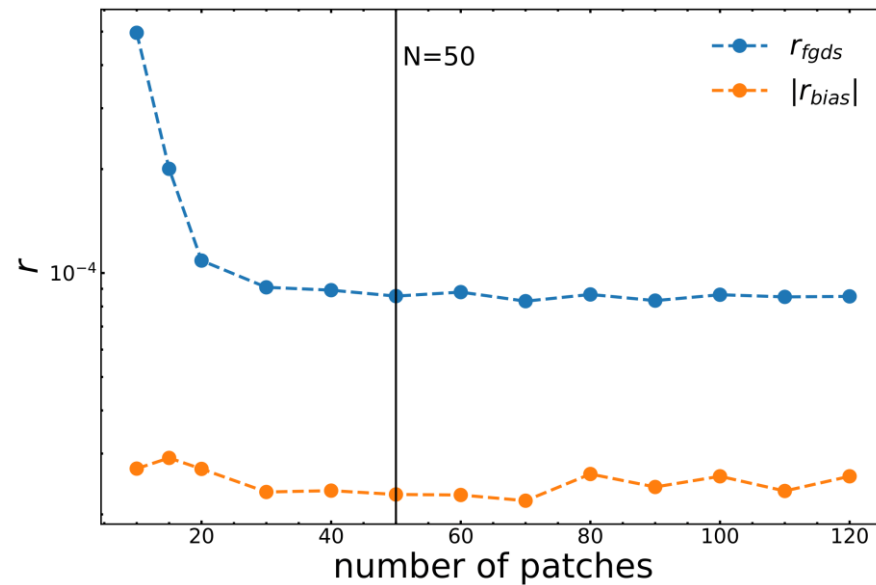
$$a_{\ell m}^B = a_{\ell m}^B \cdot \sqrt{(\ell + 2)! / (\ell - 2)!}$$



3. NUMBER OF PATCHES

CMB reconstruction bias:

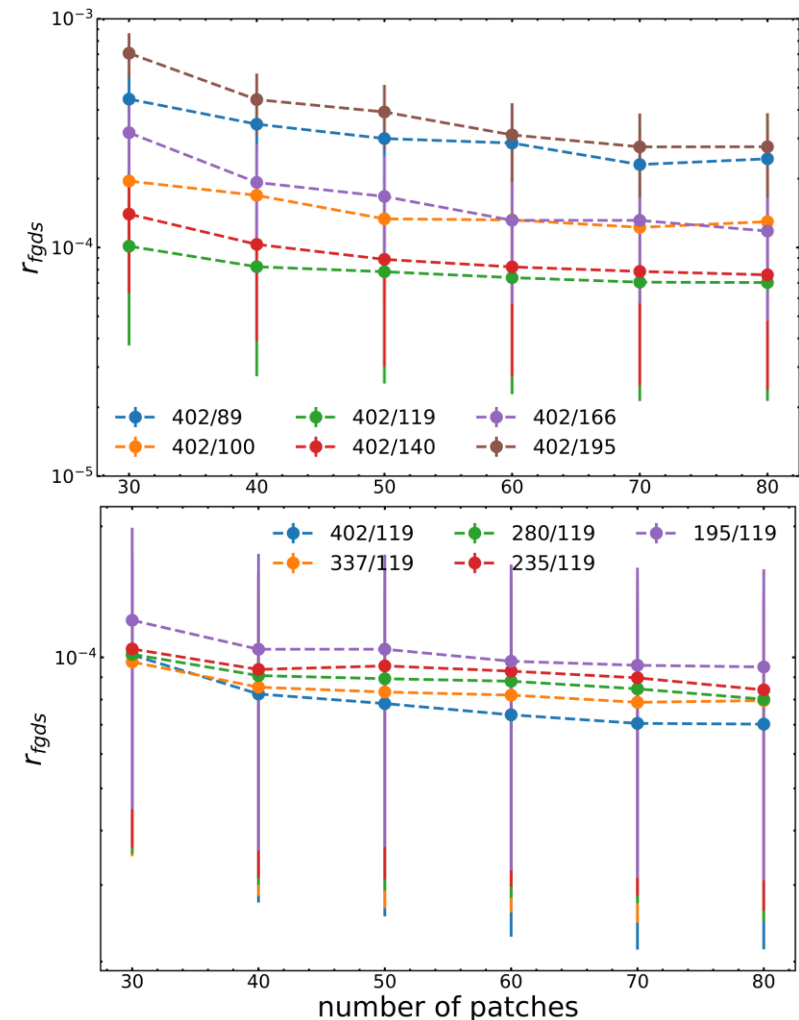
$$C_\ell^{\text{bias}} = C_\ell^{\text{out}} - C_\ell^{\text{lens}} - C_\ell^{\text{fgds}} - C_\ell^{\text{noi}}$$



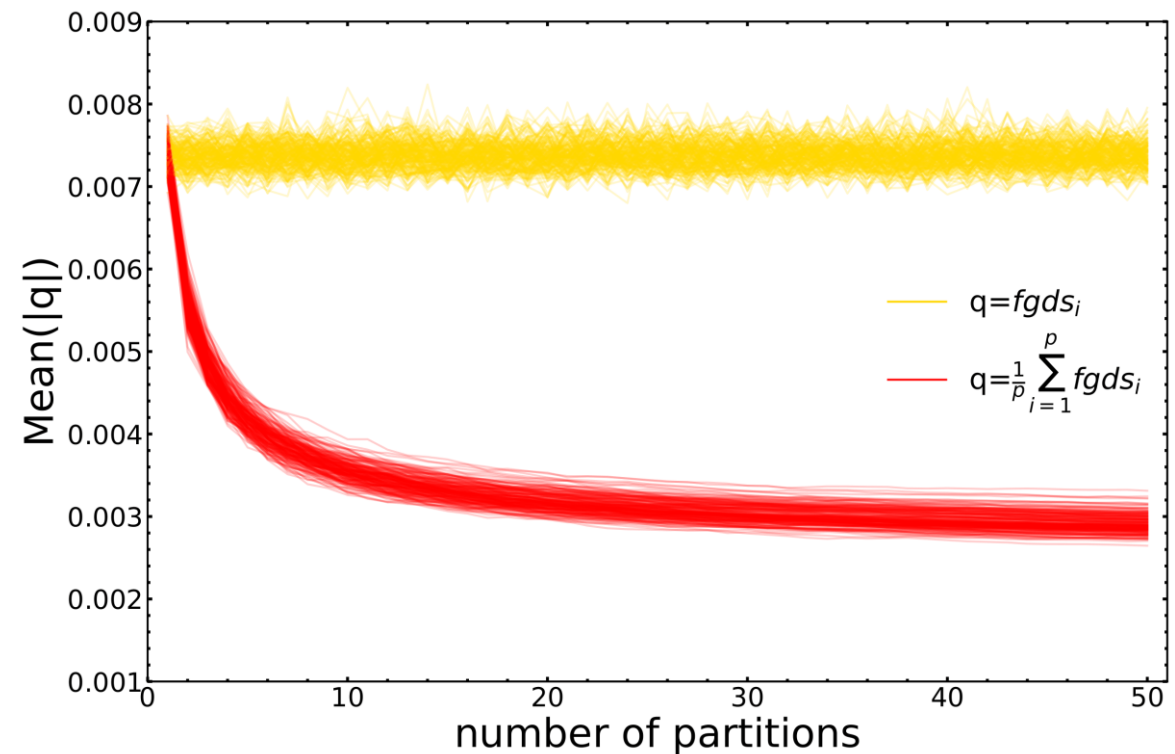
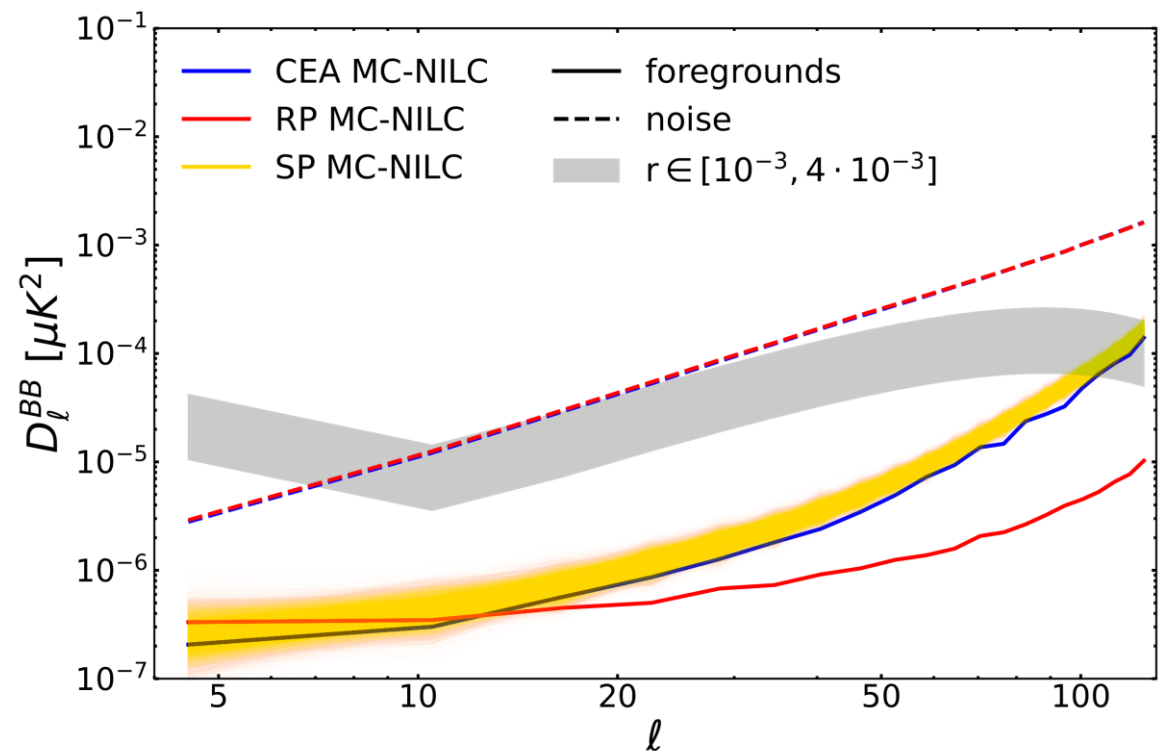
Solution to the CMB bias:

The computation of the covariance in each point excludes the point itself and a circular region around it (Coulton et al., in prep)

4. FREQUENCIES

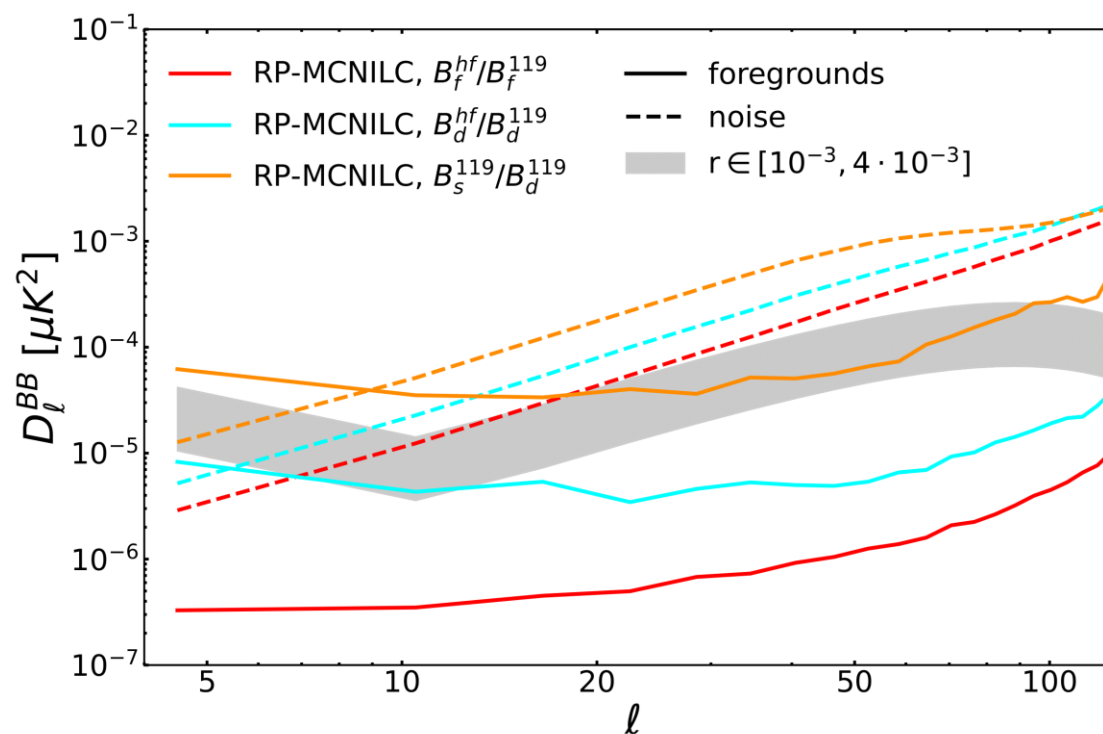


CEA VS RP

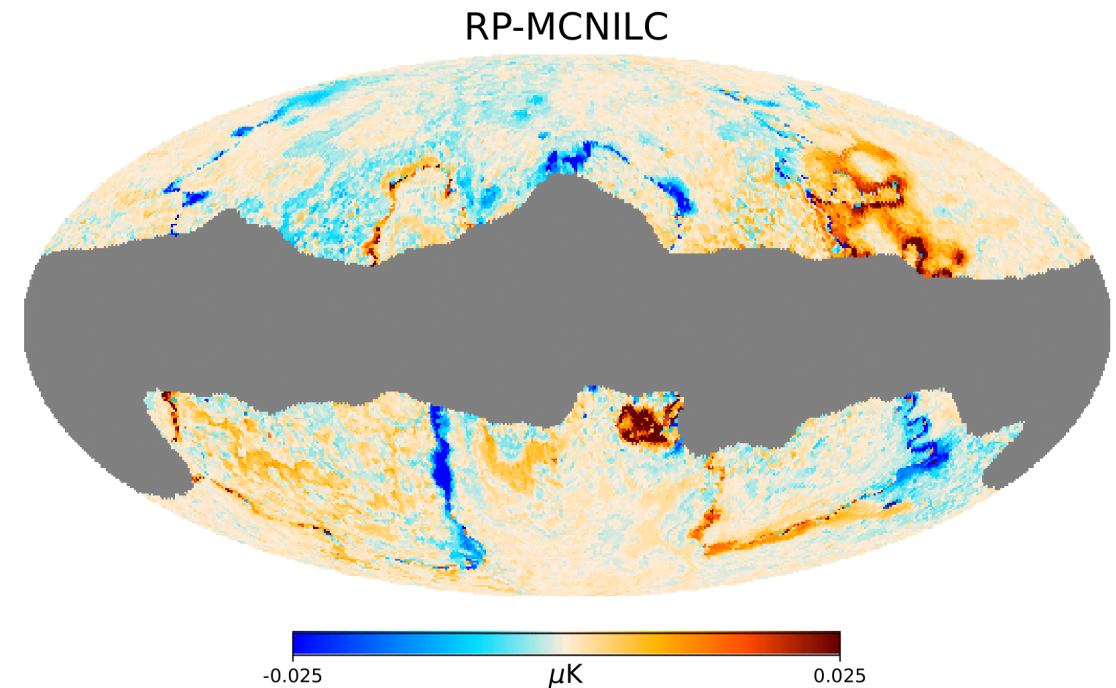
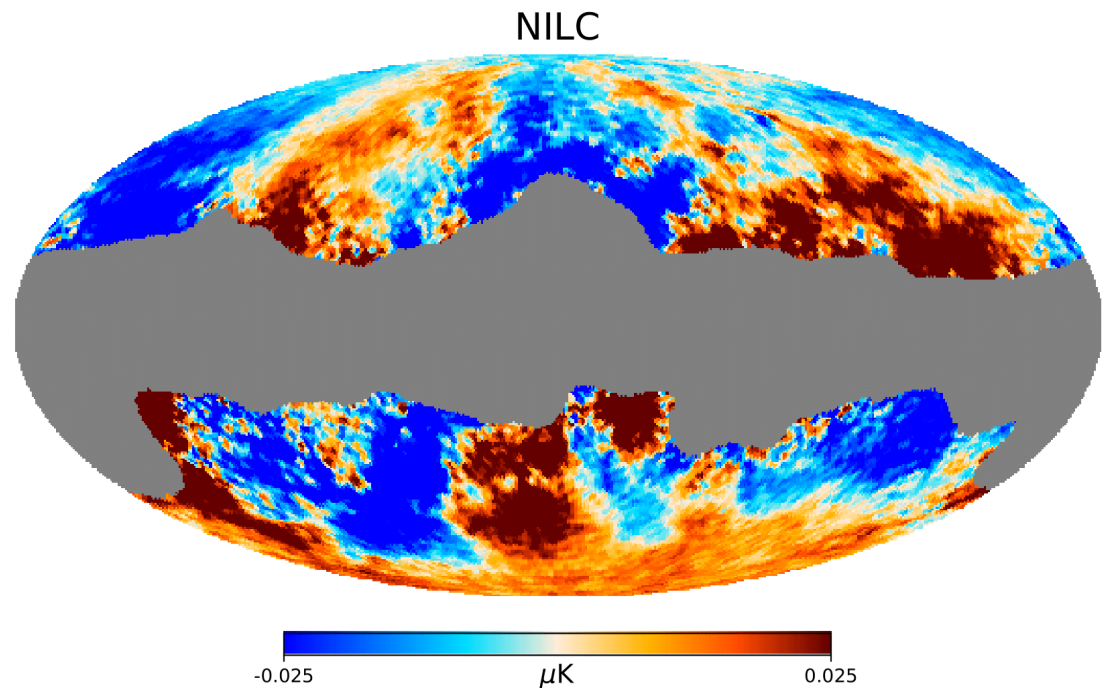


MC-NILC RATIOS

$$\frac{B_{fgds}^{337}}{B_{fgds}^{119}} = \frac{B_{dust}^{337} + B_{sync}^{337}}{B_{dust}^{119} + B_{sync}^{119}} = \frac{B_{dust}^{337}}{B_{dust}^{119}} \cdot \frac{1 + \frac{B_{sync}^{337}}{B_{dust}^{337}}}{1 + \frac{B_{sync}^{119}}{B_{dust}^{119}}}$$



Foregrounds residuals



Generalized NILC (GNILC)

At each needlet scale:

$$\widehat{\mathbf{R}}_N^{-1/2} \widehat{\mathbf{R}} \widehat{\mathbf{R}}_N^{-1/2} =$$

$$\left[\mathbf{U}_S \middle| \mathbf{U}_N \right] \cdot \begin{array}{c} \lambda_1 + 1 \\ \dots \\ \lambda_m + 1 \end{array} \left[\begin{array}{c} \\ \hline \mathbf{I} \end{array} \right] \cdot \begin{bmatrix} \mathbf{U}_S^T \\ \mathbf{U}_N^T \end{bmatrix}$$

(Remazeilles et al., 2011)

$$\widehat{\mathbf{R}}_N^{-1/2} \widehat{\mathbf{R}} \widehat{\mathbf{R}}_N^{-1/2} = \mathbf{U}_S \mathbf{D}_S \mathbf{U}_S^T + \mathbf{U}_N \mathbf{U}_N^T$$

where

$$\mathbf{D}_S = \text{diag}[\lambda_1 + 1, \dots, \lambda_m + 1]$$

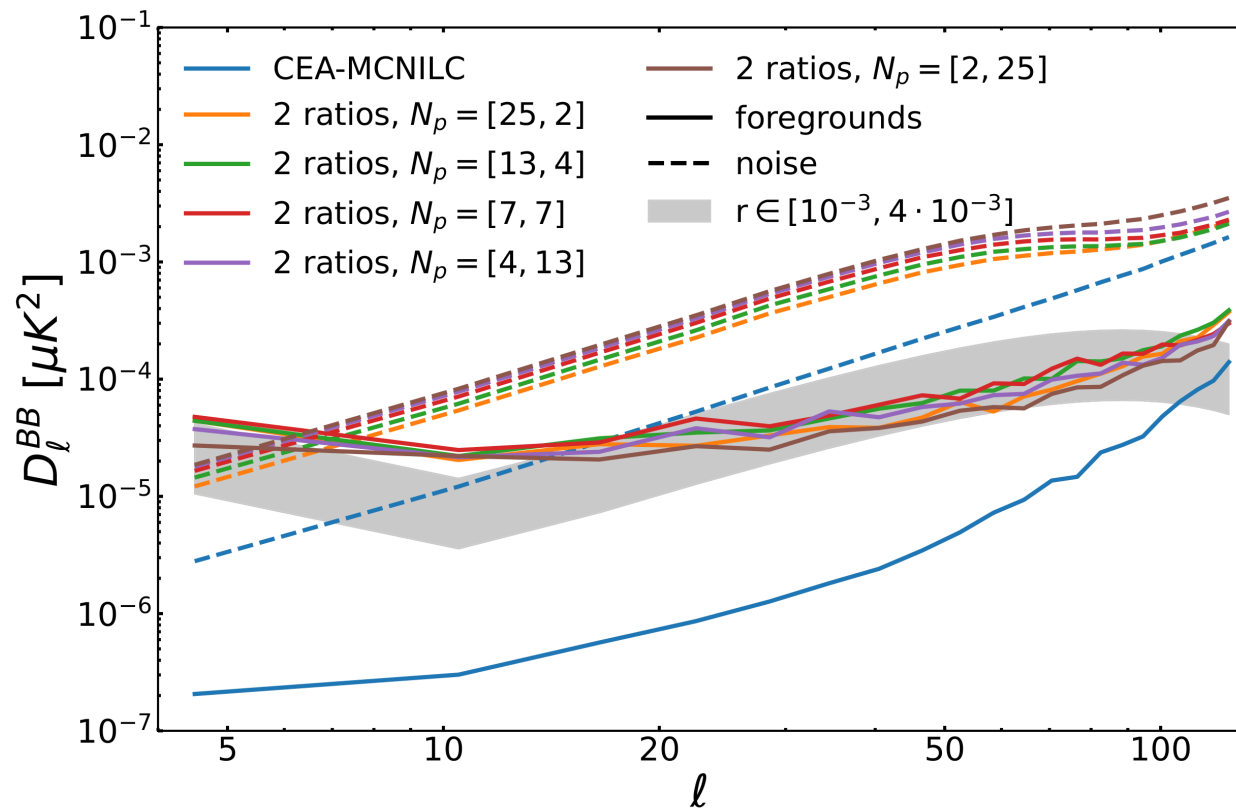
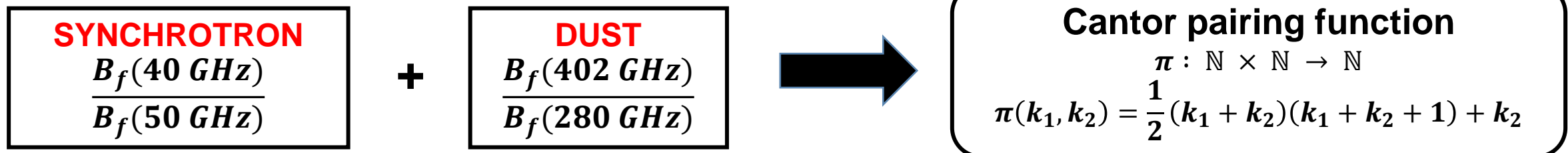


$$\begin{aligned}\widehat{\mathbf{R}}_f &= \widehat{\mathbf{R}} - \widehat{\mathbf{R}}_N \\ &= \widehat{\mathbf{R}}_N^{1/2} \left(\widehat{\mathbf{R}}_N^{-1/2} \widehat{\mathbf{R}} \widehat{\mathbf{R}}_N^{-1/2} - \mathbf{I} \right) \widehat{\mathbf{R}}_N^{1/2} \\ &= \widehat{\mathbf{R}}_N^{1/2} \left(\mathbf{U}_S (\mathbf{D}_S - \mathbf{I}) \mathbf{U}_S^T \right) \widehat{\mathbf{R}}_N^{1/2}.\end{aligned}$$

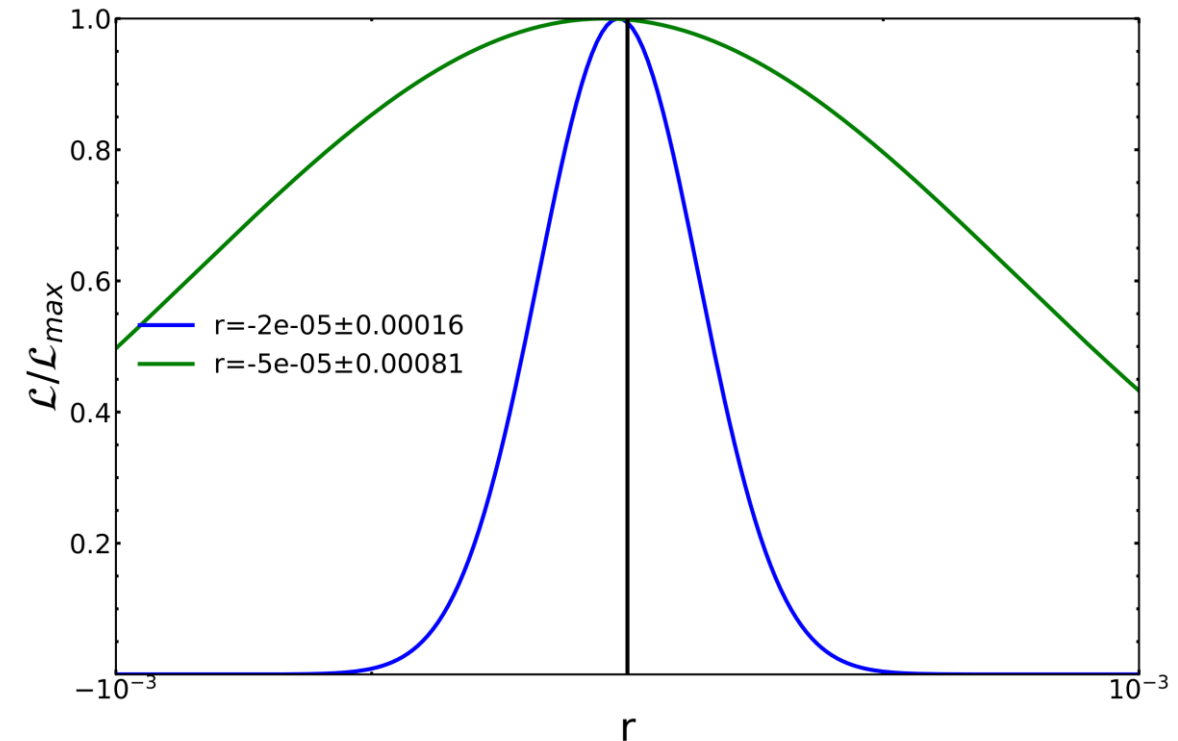
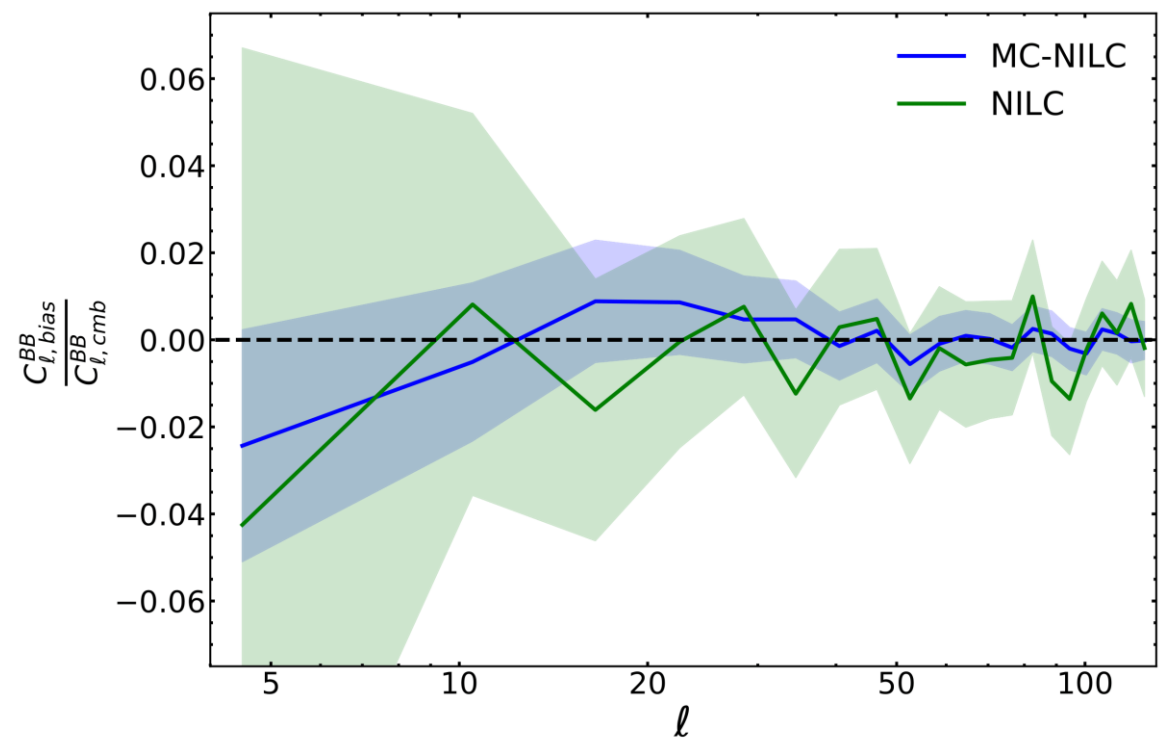
$$\widehat{\mathbf{F}} = \widehat{\mathbf{R}}_N^{1/2} \mathbf{U}_S$$

$$\mathbf{W} = \mathbf{F} \left(\mathbf{F}^T \widehat{\mathbf{R}}^{-1} \mathbf{F} \right)^{-1} \mathbf{F}^T \widehat{\mathbf{R}}^{-1}$$

MC-NILC RATIOS



BIAS in MC-NILC



SEMI-BLIND APPROACH

In case of no significant deviations of thermal dust emission from a MBB, given the LiteBIRD sensitivity, we develop an alternative semi-blind method to build the ratio

HIGH-FREQUENCY TEMPLATE : GNILC

CMB-CHANNEL TEMPLATE :

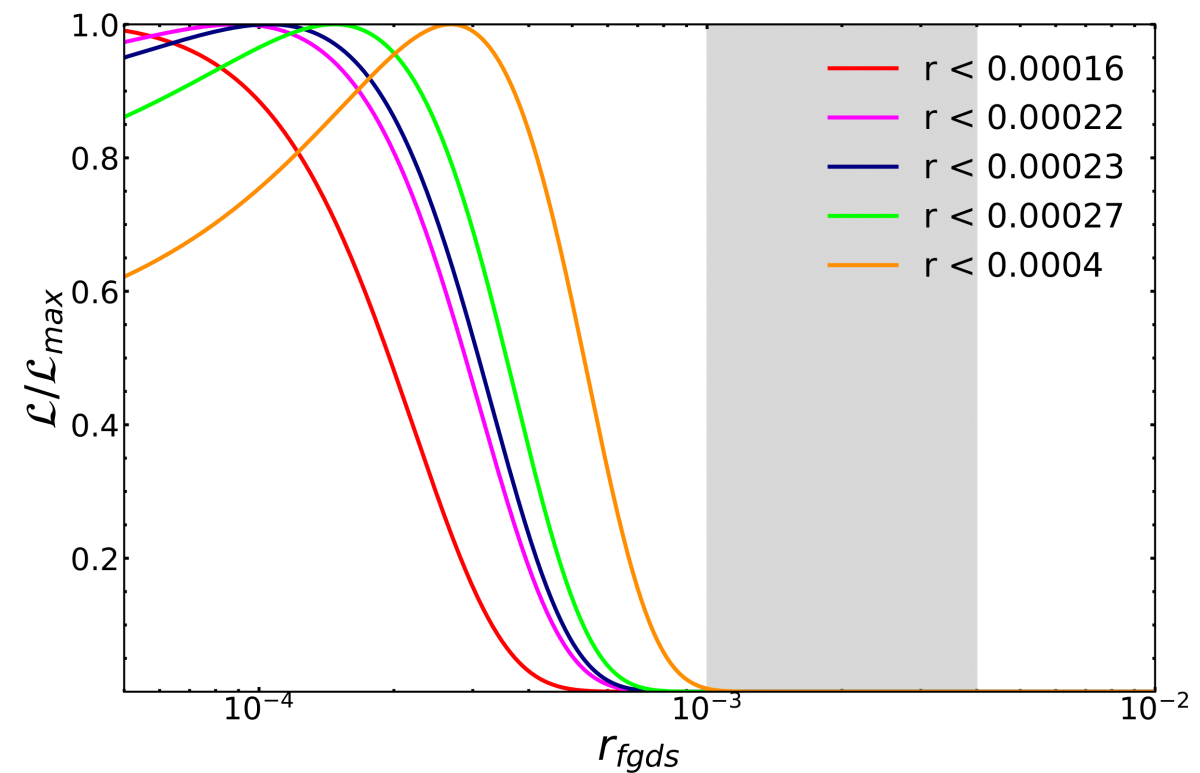
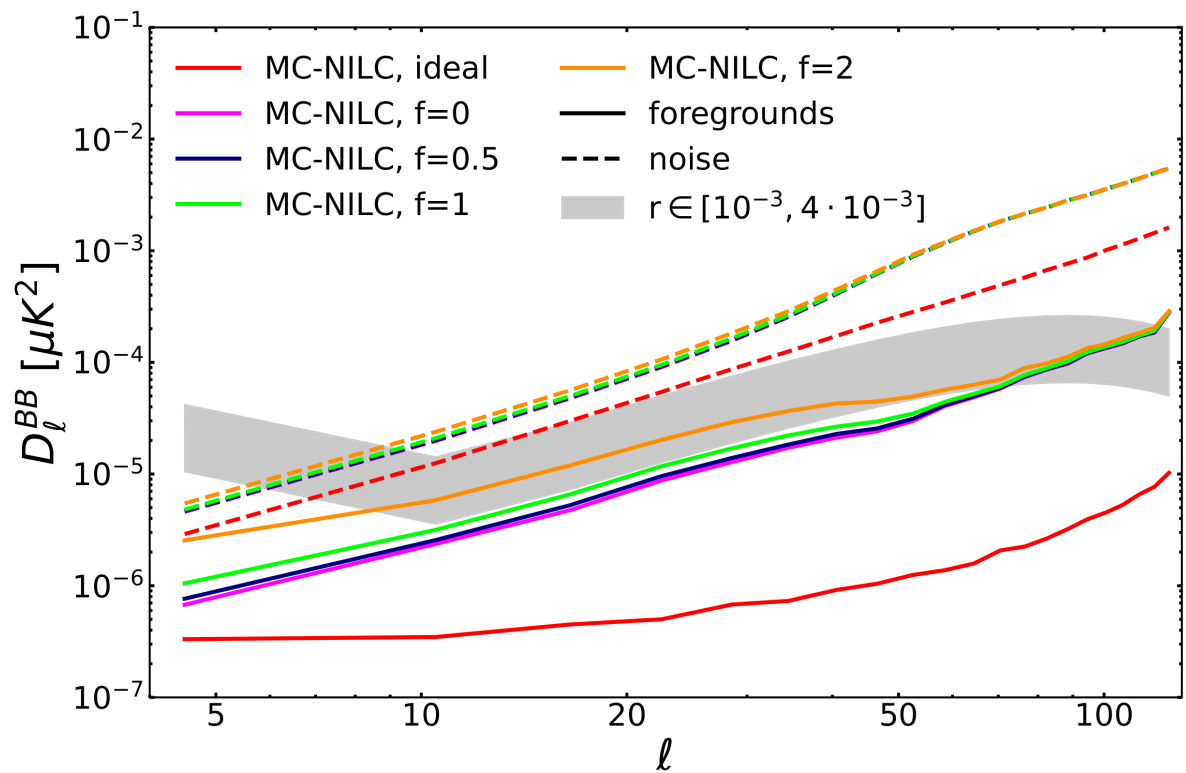
- i. LiteBIRD full QU maps at 40 and 337 GHz considered as synchrotron and dust templates
- ii. Lower noise and CMB contamination at 40 GHz with the application of cPILC on the LiteBIRD QU data
- iii. Re-scale these maps with the mis-modeled "d1s1" spectral indices to the frequency of interest
- iv. Add the two obtained QU templates and compute the corresponding B-modes map

MIS-MODELED SPECTRAL INDICES

$$\hat{X} = X + f \cdot W(\sigma(X)), \quad \text{with } X = \{\beta_d, \beta_s, T_d\} \text{ and } f = [0, 0.5, 1, 2]$$

SEMI-BLIND APPROACH

In case of no significant deviations of thermal dust emission from a MBB, given the LiteBIRD sensitivity, we develop an alternative semi-blind method to build the ratio



FULL COMPARISON

